Hydrogen Production from Aluminum-Water Reactions Subject to High Pressure and Temperature Conditions

by

Kelsey Carolyn Seto

Submitted to the Department of Mechanical Engineering
in partial fulfillment of the requirements for the degree of

Master of Science in Mechanical Engineering

at the

MASSACHUSETTS INSTITUTE OF TECHNOLOGY

June 2017

Author ..... Signature redacted .....
Department of Mechanical Engineering
May 12, 2017

Certified by..... Signature redacted .....
Douglas P. Hart
Professor of Mechanical Engineering
Thesis Supervisor

Accepted by ..... Signature redacted
Rohan Abeyaratne
Chairman, Committee on Graduate Students

Hydrogen Production from Aluminum-Water Reactions Subject to High Pressure and Temperature Conditions

by

Kelsey Carolyn Seto

Submitted to the Department of Mechanical Engineering
on May 12, 2017, in partial fulfillment of the
requirements for the degree of

Master of Science in Mechanical Engineering

Abstract

Aluminum fuel has become an attractive form of energy storage in recent years as it is both a highly abundant and extremely energy dense material. Research has discovered methods of treating aluminum with liquid metal, enabling the aluminum to produce large amounts of hydrogen when oxidized by liquid water. When this fuel reacts with water, it produces hydrogen, heat, and aluminum hydroxide ($Al(OH)_3$). Although this aluminum fuel has already been integrated into an effective mobile hydrogen production source for hydrogen fuel cells, the system size and weight is restricted by the amount of water that is required to react the aluminum. The less water that needs to be carried on board, the better, and the only way to decrease the amount of water that is required to produce hydrogen through aluminum-water reactions is to alter the chemistry of the reaction. This thesis investigates the possibility of manipulating the chemistry of these reactions at high pressures and temperatures to produce aluminum oxyhydroxide ($AlOOH$) or aluminum oxide (Al_2O_3), both of which are byproducts of aluminum-water reactions which consume less water than the $Al(OH)_3$ reaction for the amount of hydrogen produced.

A MATLAB simulation was constructed to predict the favorability of each byproduct by analyzing the Gibbs free energy of the reactions as a function of pressure and temperature. This simulation revealed that $AlOOH$ becomes favorable over $Al(OH)_3$ at $142.38°C$ and $387kPa$ and Al_2O_3 becomes favorable over $AlOOH$ at $174.21°C$ and $889kPa$ in a system with a $200ml$ volume in which $5g$ of fuel is reacted. Pressurized tests were also carried out and the experiment results showed that $AlOOH$ was produced from these aluminum-water reactions at $181°C$ and $1035kPa$, proving that it is possible to manipulate these reactions to improve the performance of aluminum fuel as a hydrogen source.

Thesis Supervisor: Douglas P. Hart
Title: Professor of Mechanical Engineering

Acknowledgments

First and foremost, I would like to thank all of my friends and family for supporting me throughout my entire MIT career. It has been a bit of a rough ride but you have always kept my spirits high and kept me believing that I could accomplish something great for myself.

To Doug Hart, thank you for your mentorship and guidance, but more importantly, for being a fun advisor. I have really enjoyed my time in your lab and maybe one day I will even be back for that PhD.

I would also like to thank my labmates Mark, Brandon, Thanasi, Jonny, Jorge and Marc for teaching me the ropes of grad school and research life, answering all of my pesky questions, suggesting design ideas when my brain was fried, and putting up with my constant complaining.

To Mark Belanger, thank you for helping me bring my setup designs to life and for turning me into a better machinist. I know that endlessly machining stainless steel isn't all that pleasant, but it was all worth it in the end and I'm very grateful to have had such a patient mentor to lead me through it all.

A huge thank you goes out to those who worked so hard to find me a suitable space for running my experiments. Without the help of John Vivilecchia, Daniel Herrick, Fabiola Hernandez, Jim Doughty, Bret Dryer, and Anthony Zolnik from the MIT Mechanical Engineering Environmental Health and Safety group and Department of Aerospace Engineering, I might not have been able to complete any of my testing. It seems that the phrase "high temperature, high pressure hydrogen" scares most people away from getting involved with my thesis work, but the five of you were brave enough to believe I knew what I was doing and you gave me a chance and fought to find me testing space. For that I am extremely grateful.

To Professor Antoine Allanore, Dr. Charlie Settens, and Tim McClure from the MIT Materials Science and Engineering Department, thank you for taking the time and having the patience to sit down with me to discuss my experiment and to help me understand my results.

I extend my most sincere gratitude to Brian Chmielowiec from the Materials Science and Engineering Department. Brian, you were my savior when my memory of freshman year chemistry was failing me and you were my guide when I was completely lost trying to figure out why my code was not aligning with my chemistry. You went out of your way to help me when you could tell I was struggling, and I really could not have finished this thesis without you. Thank you for going above and beyond, and best of luck with your PhD.

And, of course, thank you to the Insititvte for shaping me into the person I am today.

Contents

1 Introduction **15**

1.1 Hydrogen as an Energy Source 16

1.1.1 The Current State of Hydrogen Energy 16

1.1.2 Alternative Hydrogen Sources 19

1.2 Aluminum as a Hydrogen Source 20

1.2.1 Treated Aluminum Fuel for Aluminum-Water Reactions 21

1.2.2 Comparison to Compressed Hydrogen 23

1.3 Aluminum-Water Reaction Byproducts 24

2 Computational Analysis **29**

2.1 Modeling Reaction Favorability 29

2.2 Adapting Model to Real Conditions 30

2.2.1 Factoring in Nitrogen 32

2.2.2 Factoring in Steam 33

2.2.3 Final Modeling Method 34

2.3 Modeling Results and Conclusion 37

3 Pressurized Testing **41**

3.1 Test Objectives 41

3.2 Testing Setup 42

3.2.1 Functional Requirements & Design Considerations 42

3.2.2 System Design 44

3.3 Testing Process 49

3.3.1 Fuel Preparation 49
3.3.2 Reaction 49
3.4 Results 51
3.4.1 Infrared Spectroscopy 52
3.4.2 X-Ray Diffraction 55
3.4.3 Summary 58

4 Discussion and Outlook **61**
4.1 Conclusion 61
4.2 Future Testing 62
4.2.1 Testing Improvements 62
4.2.2 System Outlook 63

A Figures **65**

B Tables **71**

C Equations **73**

List of Figures

1-1 A graphical representation of where hydrogen energy storage technology stands now in terms of the DOE's 2020 goals [23] 17

1-2 Energy densities of select materials [1] 18

1-3 Comparison of volume requirements for various hydrogen storage sources required to compete with gasoline energy capacity [7] 19

1-4 Untreated aluminum fuel [22] 22

1-5 Aluminum fuel treated with gallium/indium eutectic through Slocum process [22] 22

1-6 Transformation conditions between various species of aluminum oxide crystals [8] 25

1-7 Predicted oxidized aluminum formation temperatures [12] 26

2-1 Simulated ΔG favorability for each of the three aluminum-water reactions as a function of temperature at atmospheric pressure 37

2-2 Simulated ΔG favorability for each of the three aluminum-water reactions as a function of temperature at operating pressure $550kPa$ . . . 38

2-3 Simulated ΔG favorability for each of the three aluminum-water reactions as a function of temperature at operating pressure $3000kPa$ . . 38

2-4 Graph of simulated byproduct transition conditions 40

3-1 Full test system setup 44

3-2 Main body of the test setup 46

3-3 4-bar mechanism initiation actuator 47

3-4 Relief valve and pressure fail-safe 48

3-5 Reaction setup model 50

3-6 Reaction setup cross-section: 1) nitrogen pre-pressurizes the setup 2) pressure transducer detects the pressure 3) fuel drops into water below 4) relief valve expels nitrogen, steam and hydrogen 50

3-7 Images of oxidized aluminum byproducts from testing. Top row, left to right: atmospheric pressure, $1035kPa$, $1725kPa$. Bottom Row, left to right: $3450kPa$, $5170kPa$, $6900kPa$ 52

3-8 FTIR analysis results representing the absorbance spectrum for $Al(OH)_3$ produced by aluminum-water reactions carried out under standard atmospheric conditions 54

3-9 FTIR analysis results representing the absorbance spectra of the byproducts of the pressurized aluminum-water reaction tests 54

3-10 X-Ray diffraction peaks from the 1035kPa pressurized aluminum-water reaction compared to known $Al(OH)_3$ diffraction pattern 55

3-11 X-Ray diffraction peaks from the 1035kPa pressurized aluminum-water reaction compared to known $AlO(OH)$ diffraction pattern 56

3-12 X-Ray diffraction peaks from the 1725kPa pressurized aluminum-water reaction compared to known $AlO(OH)$ diffraction pattern 56

3-13 X-Ray diffraction peaks from the 3450kPa pressurized aluminum-water reaction compared to known $Al(OH)_3$ diffraction pattern 57

3-14 X-Ray diffraction peaks from the 3450kPa pressurized aluminum-water reaction compared to known $AlO(OH)$ diffraction pattern 57

3-15 X-Ray diffraction peaks from the 5170kPa pressurized aluminum-water reaction compared to known $AlO(OH)$ diffraction pattern 58

3-16 X-Ray diffraction peaks from the 6900kPa pressurized aluminum-water reaction compared to known $AlO(OH)$ diffraction pattern 58

A-1 Calculated FTIR absorbance spectra for various OH bonds found in aluminum oxyhydroxide crystalline structures [24] 65

A-2 Documented x-ray diffraction spectra for $AlOOH$ [18] 66

A-3 Close up image of reaction initiation actuator 67
A-4 Close up image of initiation and fail safe mechanisms together 68
A-5 Heat recovery systems proposed in [26] 69

THIS PAGE INTENTIONALLY LEFT BLANK

List of Tables

1.1 Comparison of chemical hydride hydrogen storage potential to hydrogen storage potential of aluminum [22] 20

2.1 Temperatures at which $AlOOH$ becomes more favorable than $Al(OH)_3$ and at which Al_2O_3 becomes more favorable than $AlOOH$ at different pressure conditions compared to the boiling point of water at that pressure 39

3.1 Functional Requirement Specifications 43

3.2 Test specific notes from running the pressurized aluminum-water reactions in the MIT blast chamber 53

B.1 U.S. Department of Energy's reported current state of hydrogen energy and goals for hydrogen energy [5] 71

B.2 Reaction data for hydrothermal oxidation of aluminum to create $AlOOH$ in a very small scale production study [21] 71

B.3 Variables used in Chapter 2 72

THIS PAGE INTENTIONALLY LEFT BLANK

Chapter 1

Introduction

As modern power systems transition away from fossil fuels and towards alternative energy sources, a major problem is becoming evident: most alternative fuels are significantly more expensive and less energy dense than oil, making it very difficult to sensibly replace fossil fuels. For instance, removing the combustion engine and gasoline tank from a car and replacing those parts with electric motors and lithium-ion batteries without altering the initial volume or weight of the car will result in a vehicle that can only travel a fraction of the distance. Increasing the energy density of rechargeable batteries is a pricey endeavor because doing so typically involves using less abundant and therefore more expensive materials for anodes and cathodes [17].

Hydrogen fuel cell technology is another energy technology that is being actively developed and implemented in systems such as unmanned underwater vehicles (UUVs). These fuel cells have high efficiencies and hydrogen gas can be produced simply through electrolysis; however, even when hydrogen is compressed to extremely high pressures, the energy density of the gas still cannot compete with that of fossil fuels. Additionally, the process of handling and storing hydrogen is both energy intensive and dangerous because compressing hydrogen to high pressures requires a hefty amount of pumping power and the gas itself is explosively combustible in the presence of oxygen gas. These issues are driving factors for research into different hydrogen sources for fuel cell technology.

In recent years, aluminum has been proposed and successfully tested as a hydro-

gen production fuel because the combination of raw aluminum with water produces hydrogen gas and an inert oxidized aluminum byproduct. There are two proven methods of carrying out this reaction for the purpose of producing hydrogen gas. The first involves raising and maintaining the temperature of the aluminum above its melting point and running water over the molten metal [26]. The second involves pre-treating the aluminum with a eutectic to bypass the oxide layer that typically forms on the surface of the aluminum and which renders the aluminum relatively unreactive as it is seen in day-to-day life [14, 22]. This pre-treated aluminum fuel then reacts violently with water to produce hydrogen gas, heat, and aluminum hydroxide ($Al(OH)_3$) without the need of an outside heat source.

This thesis aims to explore the potential of reacting gallium-indium-treated aluminum fuel with water in high pressure, high temperature environments to manipulate the production of aluminum oxyhydroxide ($AlOOH$) and aluminum oxide (Al_2O_3), which are dehydrated forms of aluminum hydroxide ($Al(OH)_3$), and therefore reduce the amount of water reactant required to produce hydrogen, increasing the overall energy density of the system.

1.1 Hydrogen as an Energy Source

1.1.1 The Current State of Hydrogen Energy

Hydrogen is a very attractive form of energy storage for three main reasons: 1) it has an extremely high gravimetric energy density, 2) hydrogen gas production is a straightforward and inexpensive process and can store energy from renewable energy sources such as solar and wind if produced through electrolysis, and 3) the entire cycle of producing hydrogen and running it through a fuel cell can be environmentally friendly as the cycle involves only hydrogen, oxygen and water. Additionally, hydrogen fuel cells have relatively high energy efficiencies ranging between 40% and 60% and developments to incorporate cogeneration have proven that this number can climb as high as 85%. Comparatively, internal combustion engines have efficiencies of

about 35%. In order to make effective use of hydrogen fuel cells in vehicles, however, an on board hydrogen source needs to flow hydrogen gas through the fuel cell on demand. This poses a complicated challenge because hydrogen gas is not only a dangerous and explosive gas to store in vehicles that are prone to impact and collision but it must also be heavily compressed in order to store a significant amount of energy in a compact on board space. Figure 1-1 below depicts the Department of Energy's goals for hydrogen energy technology in the year 2020. It is clear that, although most of the functional requirements of hydrogen energy systems have already been met, there are still major improvements mainly surrounding hydrogen energy storage systems' energy density that need to be made to before hydrogen can become a competitive form of energy storage [3].

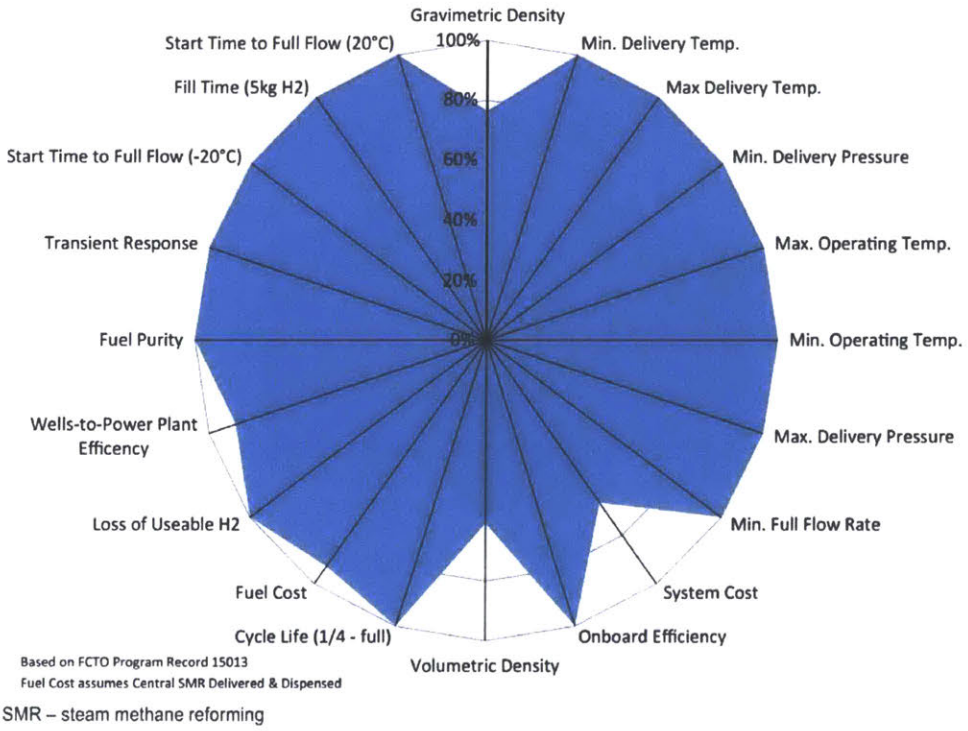

Figure 1-1: A graphical representation of where hydrogen energy storage technology stands now in terms of the DOE's 2020 goals [23]

Uncompressed hydrogen gas has a volumetric energy density of only $0.01 MJ/L$ compared to gasoline's $34.2 MJ/L$, and even when in liquid form, hydrogen's volumetric energy density is still less than 30% of that of gasoline as seen in Figure

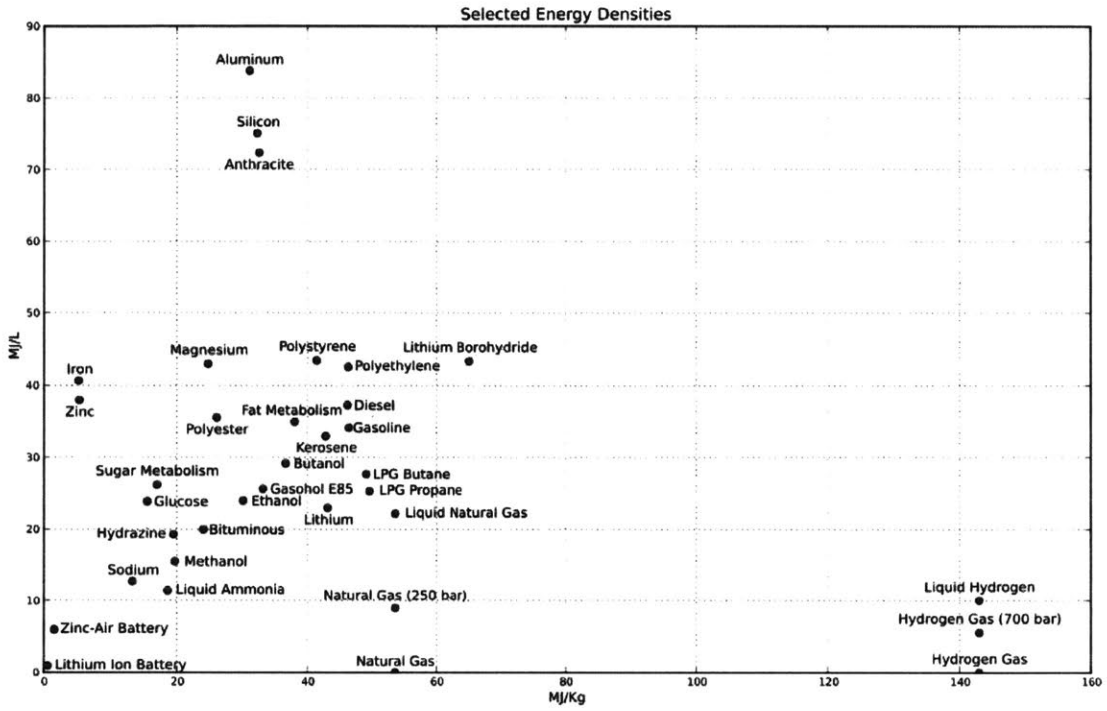

Figure 1-2: Energy densities of select materials [1]

1-2. As such, storing enough hydrogen in a volume that is compact enough to be mobile requires compression and/or cooling, increasing the overall cost of hydrogen energy and increasing the weight of the system. This in turn significantly impacts the gravimetric energy density of the system which should be a huge benefit of hydrogen fuel seeing as it has a gravimetric energy density of $147MJ/kg$ (compared to that of gasoline at $46.4MJ/kg$). Ultimately, hydrogen's extremely low volumetric energy density prevents it from meeting either of its energy density goals. Processing also decreases the overall efficiency of hydrogen gas energy storage since energy is required to compact the gas, decreasing the net potential energy of hydrogen gas per unit of energy applied to the system to make hydrogen gas a viable energy storage method.

For this reason, some argue that a hydrogen fuel economy is impractical because, once the efficiency of electrolysis, energy costs of compression/liquefaction, energy costs of transportation, and efficiency of hydrogen fuel cells are all taken into account, only about 25% of the initial energy fed into the system is available to do work [9, 10]. The majority of these losses are derived from production, storage and transportation

and can be reduced by developing more convenient hydrogen sources [15].

1.1.2 Alternative Hydrogen Sources

One method of reducing the energy losses accrued through the production and compression/liquefaction of hydrogen gas is that of storing hydrogen potential in other chemicals and materials. Chemical hydrides have become a popular area of research for hydrogen storage because they store hydrogen atoms in a solid form and will readily oxidize in water, releasing those hydrogen atoms as hydrogen gas and running that gas into a fuel cell on demand. As depicted in Figure 1-3, this chemical storage mechanism drastically improves the volumetric energy density of the hydrogen source, although it is still not quite as effective as using liquid hydrogen. The added benefit over liquid hydrogen, however, is the fact that chemical hydrides also improve gravimetric energy density of the system as heavy tanks are no longer required for containment.

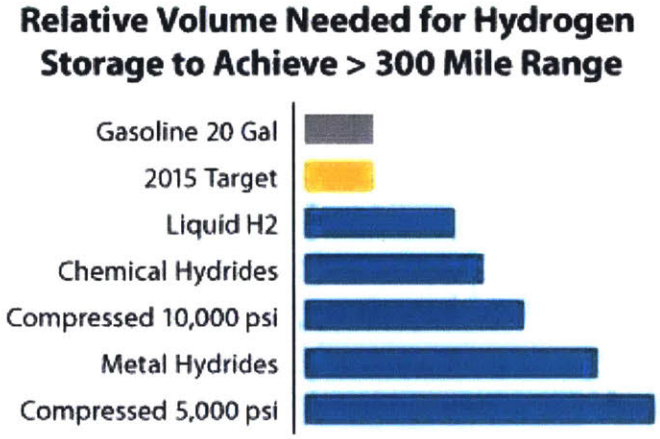

Figure 1-3: Comparison of volume requirements for various hydrogen storage sources required to compete with gasoline energy capacity [7]

$NaBH_4$, KBH_4, LiH, NaH, and MgH_2 are some of the chemical hydrides that are used for hydrogen storage and are very reactive in water [11]. Of these, $NaBH_4$ has been found to be the most favorable because it yields the most hydrogen gas for the amount of reactant and water required while also doing so at a reasonable cost. Reasonable cost, however, is a relative when considering chemical hydrides. The

	Aluminum	Sodium Borohydride (NaBH4)	Calcium Hydride (CaH2)	Lithium Borohydride (LiBH4)
Hydrogen Produced at STP (Liters)	1	1	1	1
Moles of Reactant	0.030	0.011	0.022	0.011
Mass of Water Consumed	1.61	0.40	0.80	0.80
Density (g/cc)	2.7	1.07	1.7	0.66
Liters of Material Required (mL or cc)	0.297	0.395	0.553	0.368
Cost of material ($/kg)	2	600	500	1500
Cost (dollars/Liters of H2)	0.002	0.253	0.470	0.365

Table 1.1: Comparison of chemical hydride hydrogen storage potential to hydrogen storage potential of aluminum [22]

current cost of hydrogen per liter of STP gas is $\$0.050/L$ when pressurized to $700bar$ and $\$0.039/L$ when pressurized to $350bar$. The DOE's target price for hydrogen in the year 2020 is $\$0.030/L$ and $\$0.024/L$ in the long term [5]. As seen in Table 1.1, the cost of using $NaBH_4$ for hydrogen storage is still five times the current cost of hydrogen gas pressurized to $700bar$ and ten times the cost of the DOE's long term target price for hydrogen storage.

1.2 Aluminum as a Hydrogen Source

Looking back at Figure 1-2, aluminum has the highest volumetric energy density of all of the energy fuels listed. With a preferred oxidation state of 3^+, aluminum readily oxidizes from its elemental form, giving it significant energy storage potential. It is also conveniently the most abundant metal found in the Earth's crust. Generally speaking, aluminum that we encounter everyday is inert and appears to have little potential as a fuel; however, this is merely due to the fact that aluminum is so reactive that it oxides readily with the oxygen in its surroundings, enveloping it in a layer of aluminum oxide (Al_2O_3). This outer layer is inert and passivates the raw aluminum, preventing it from reacting violently with oxidizing agents such as water.

Recent developments have proven effective at penetrating the oxide layer that builds up on the surface of the aluminum, allowing the raw aluminum underneath to be accessed. Once water gets past the oxide layer, it can continuously oxidize the raw aluminum to near reaction completion, releasing large amounts of hydrogen gas. A preferred oxidation state of 3^+ renders aluminum capable of reducing 3 hydrogen ions or $\frac{3}{2}$ moles of diatomic hydrogen gas per mole of aluminum reacted.

The acid etching process and the Woodall process are two methods that have proven successful in breaking through aluminum's oxide layer and accessing this oxidation potential for hydrogen production. The first of these processes involves the reaction of aluminum in strong acids to constantly break down the oxide layer that forms and the second involves the dissolution of aluminum in liquid gallium to prevent the oxidation of the aluminum by air instead of water. Although both of these methods are effective, neither is ideal for creating a mobile hydrogen production system for fuel cells. Acid etching requires large quantities of strong acids which are dangerous to handle, and the Woodall process requires a bath of gallium, a material that is both heavy and expensive [22].

1.2.1 Treated Aluminum Fuel for Aluminum-Water Reactions

A third process has been developed at MIT by researcher Jonathon Slocum over the past three years. Similar to the Woodall process, this method employs liquid metal to disrupt aluminum's oxide layer, but unlike the Woodall process, minimal amounts of this gallium-indium eutectic are required to render the aluminum reactive with water. The Slocum process has been proven to achieve a 98% reaction completion percentage when reacted with water while containing only 2% gallium-indium eutectic by mass as opposed to the 97%-99.99% required by the Woodall process [22].

This large decrease in the liquid metal volume requirement is achieved by essentially baking the gallium-indium eutectic into the aluminum. When heated, the aluminum and its exterior oxide layer undergo thermal expansion, and at temperatures around $135°C$, forces caused by the increased expansion of the aluminum over the expansion of the oxide layer cause the oxide layer to crack. Normally, the exposed

Figure 1-4: Untreated aluminum fuel [22]

Figure 1-5: Aluminum fuel treated with gallium/indium eutectic through Slocum process [22]

aluminum would oxidize in the atmosphere, but when heated in a bath of liquid metal eutectic, the eutectic penetrates these cracks and is drawn into the grain boundaries of the aluminum, causing embrittlement. The aluminum fuel bakes in the eutectic until the liquid metal has had enough time to diffuse throughout the entirety of the fuel, at which point the fuel can be extracted from the bath and the excess eutectic can be removed from the fuel in a centrifuge. This produces a dry, brittle aluminum fuel that resists oxidation by air, reacts violently with water to produce hydrogen gas, and can be created in large batches.

Although aluminum fuel does not produce as much hydrogen per mole of reactant as some chemical hydrides, as seen in Table 1.1, the material is more dense than hydrides and can produce the same amount of hydrogen gas using a smaller volume of reactants. It is also important to note that chemical hydrides are significantly more expensive than aluminum. While hydrides currently cost ten times the goal price per liter of hydrogen produced, aluminum fuel, when prepared using the Slocum process, can be produced for less than $0.01 per liter of hydrogen, rendering it a very cost efficient hydrogen source that meets and exceeds the price goals set by the Department of Energy.

1.2.2 Comparison to Compressed Hydrogen

A kilogram of aluminum can produce $12.47MJ$ of energy stored as chemical energy potential in hydrogen gas produced by aluminum-water reactions. In addition to this, the redox reaction produces $15.55MJ$ of heat, yielding a total gravimetic energy density of $28.02MJ/kg_{Al}$ and a volumetric energy density of $75.67MJ/L_{Al}$. Both values are extremely close to the energy densities of elemental aluminum seen in Figure 1-2, indicating that the aluminum-water reactions convert almost all of the aluminum's chemical potential energy into forms of energy that can be harvested. These values are not however, the gravimetric and volumetric density values for the overall energy storage mechanism.

When taking into consideration the amount of water that is consumed by the reaction, the gravimetric energy density drops to $9.33MJ/kg$ - $13.71MJ/kg$ and the volumetric energy density drops to $11.81MJ/L$ - $20.06MJ/L$. While the gravimetric density of this reaction is not nearly as high as that of hydrogen ($147MJ/kg$), it is important to recognize that when all of the equipment required to store hydrogen at high pressures or in liquid form is taken into account, the gravimetric density of the hydrogen system is much lower than that of pure hydrogen gas, so it follows that the DOE's long term gravimetric energy density goal is actually only $12.8MJ/kg$ [1]. Aluminum fuel does not require complex containers or equipment, which means that a gravimetric energy density within that $9.33MJ/kg$ - $13.71MJ/kg$ range would be acceptable. The DOE's long term goal for volumetric energy density is $9.87MJ/L$ [2], which is easily achievable with the range of $11.81MJ/L$ - $20.06MJ/L$ for aluminum-water reactions.

The ranges for these energy density values are determined by the exact chemistry of the aluminum-water reaction that takes place to produce hydrogen gas. There are three possible reactions which are defined by the amount of water that they consume and the chemistry of the oxidized aluminum byproduct they produce. In the ideal scenario, the reaction that yields the most hydrogen for the least amount of water

[1] Calculated from DOE data in Table B.1
[2] Calculated from DOE data in Table B.1

consumed will occur, maximizing the energy densities for the system, but controlling that reaction is a complex process.

1.3 Aluminum-Water Reaction Byproducts

Aluminum-water reactions have three possible stable byproducts: aluminum hydroxide ($Al(OH)_3$), aluminum oxyhydroxide ($AlOOH$), and aluminum oxide (Al_2O_3). Each of these byproducts has multiple structural forms determined by crystalline structure, but for the purpose of this study, we are only concerned with overall molecular composition which indicates the ratios in which each element is present in each compound. The less hydrogen that is present in the byproduct, the better.

$$Al_{(s)} + 3H_2O_{(l)} \rightarrow Al(OH)_{3(s)} + \frac{3}{2}H_{2(g)} + Q \tag{1.1}$$

$$Al_{(s)} + 2H_2O_{(l)} \rightarrow AlOOH_{(s)} + \frac{3}{2}H_{2(g)} + Q \tag{1.2}$$

$$Al_{(s)} + \frac{3}{2}H_2O_{(l)} \rightarrow \frac{1}{2}Al_2O_{3(s)} + \frac{3}{2}H_{2(g)} + Q \tag{1.3}$$

When aluminum is oxidized by water, hydrogen atoms are released from the water molecules. These hydrogen atoms either pair and are released as diatomic hydrogen gas or remain attached to the oxygen molecule in the form of hydroxide ions and attach to the aluminum and are incorporated into the byproduct. The fewer hydrogen atoms incorporated into the aluminum byproduct, the more hydrogen gas is then produced per molecule of water as demonstrated in equations 1.1, 1.2, and 1.3. This means that Al_2O_3 is the most favorable of these three byproducts for aluminum-water reactions for hydrogen production. All three byproducts are known to be stable powders under standard temperature and pressure conditions; however, the conditions necessary to force one reaction to occur over another are unclear.

In theory, carrying out the first reaction (1.1) and dehydrating the $Al(OH)_3$ to Al_2O_3 would have the same effect as carrying out the third and most ideal reaction (1.3), producing as much hydrogen gas per mole of water reactant as possible; how-

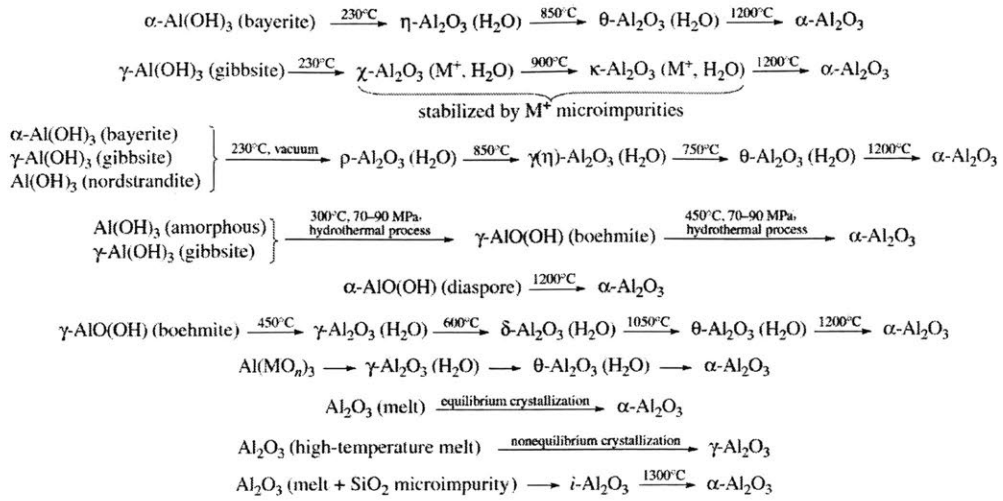

Figure 1-6: Transformation conditions between various species of aluminum oxide crystals [8]

ever, changing oxidized aluminum compound forms is an energy intensive process.

Described in Figure 1-6, converting $Al(OH)_3$ to any form of $AlOOH$ requires temperatures of $300°C$ and $70-90MPa$. Moving between $AlOOH$ and Al_2O_3 requires even more extreme conditions of $450°C$ and $70-90MPa$. These thresholds generally align with the thresholds published by the Department of Energy which states that aluminum-water reactions will yield $Al(OH)_3$ at reaction temperatures below $280°C$, $AlOOH$ at reaction temperatures between $280°C$ and $480°C$, and Al_2O_3 at reaction temperatures above $480°C$. This statement, however, is incorrect because the Gibbs free energy graph that the DOE references, Figure 1-7, depicts the change in Gibbs free energy of formation as opposed to the change in Gibbs free energy for the specific aluminum-water reaction. The two are different because each of the aluminum-water reactions that produces each respective byproduct involves different components and in different ratios than the standard formation reaction of each of the byproducts themselves. This means that Figure 1-7 is actually a graphical representation of the species stability described in Figure 1-6 as opposed to the prediction of aluminum-water reaction byproducts. The specifics on the conditions required to control the byproducts of aluminum-water reactions then remain unknown.

Due to the fact that both $AlOOH$ and Al_2O_3 have desirable properties for var-

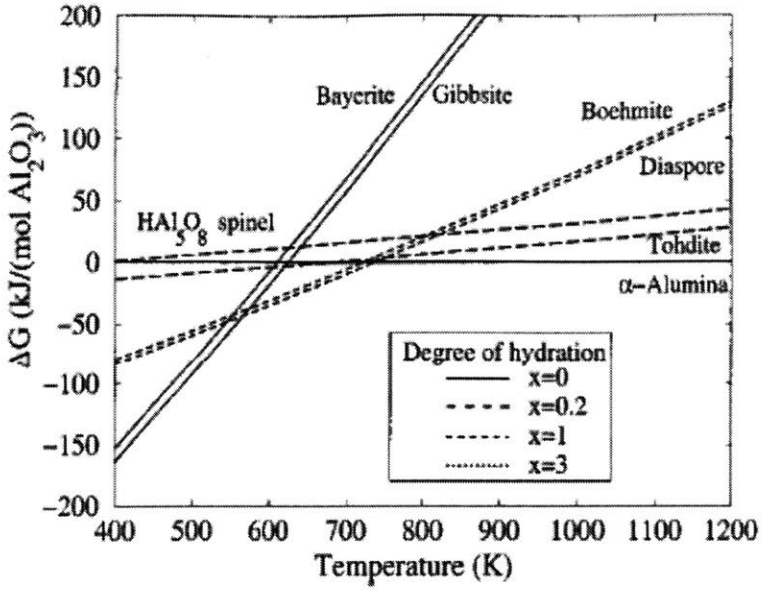

Figure 1-7: Predicted oxidized aluminum formation temperatures [12]

ious chemical applications, the chemistry world has found ways to produce these compounds for their needs. Some labs implement hydrothermal oxidation of expensively manufactured aluminum micro/nano powder to achieve the characteristics they desire, but the methods are still under development as the specific reaction operating conditions required to produce the desired product are not consistent or clearly defined.

Early experiments involved heating a mixture of fine aluminum powder and water in an autoclave heated to $250°C$ for as long as 6 hours which only produced about 30% of the expected yield of $AlOOH$ [21]. A more successful experiment mixed $4\mu m$ aluminum micropowder into a slurry with water at temperatures ranging from $230°C - 360°C$ at pressures ranging from $3MPa - 20MPa$ for about 10 minutes, producing 100% of the expected yield of $AlOOH$ [21][3].

These operating conditions are within the same order of magnitude of the conditions expected to force the dehydration of $Al(OH)_3$ to $AlOOH$, but there still are less extreme conditions that have proven to yield $AlOOH$. In one case, hol-

[3]Results of this successful experiment can be found in Figure B.2.

low nanospheres of $AlOOH$ were produced by oxidizing aluminum nanopowder with deionized water in an environment heated from $24°C$ to $60°C$ [18][4]. In one other case, $AlOOH$ microspheres were fabricated using a process other than hydrothermal oxidation of aluminum powder and were dehydrated to Al_2O_3 microspheres through calcination at temperatures ranging from $400°C$ to $800°C$ [16].

The mixed results of all of these studies merely indicate that the conditions required to manipulate aluminum-water reactions at a scale necessary to produce and feed hydrogen into a fuel cell cannot be confidently predicted without first simulating the appropriate scenario.

[4]The operating pressure for this case was not noted

THIS PAGE INTENTIONALLY LEFT BLANK

Chapter 2

Computational Analysis

2.1 Modeling Reaction Favorability

Modeling the favorability of aluminum-water reaction byproducts requires the evaluation of the Gibbs free energy of the reaction components. If the difference between the Gibbs free energy of the products and the Gibbs free energy of the reactants is negative ($\Delta G < 0$), the reaction is favorable and will occur spontaneously, and if the difference is positive ($\Delta G > 0$), the reaction is unfavorable and will not occur at all without outside influence; in fact it will proceed spontaneously in the reverse direction. A reaction without a change in Gibbs free energy ($\Delta G = 0$) is in equilibrium. This change in Gibbs free energy is defined below in equation 2.1 for a constant pressure and temperature.[1]

$$\Delta G = \Delta H - T\Delta S \tag{2.1}$$

This equation can be further broken down based on the energies and enthalpies of reactants and products in a chemical reaction and then broken down again based on the specific energies and enthalpies of the chemicals involved and the stoichiometry of the reaction, represented below by equations 2.2 - 2.4.

$$G_{products} - G_{reactants} = (H_{products} - H_{reactants}) - T_{rxn}(S_{products} - S_{reactants}) \tag{2.2}$$

[1]Refer to Table B.3 for a full description of variables.

$$G_{products} = g_{Al(OH)_3} + \frac{3}{2} \cdot g_{H_2} \tag{2.3}$$

$$G_{reactants} = g_{Al} + 3 \cdot g_{H_2O} \tag{2.4}$$

Equations 2.3 and 2.4 above represent the Gibbs free energies calculated for the $Al(OH)_3$ byproduct reaction, incorporating the reaction stoichiometry from equation 1.1 and the specific free energies of the involved chemical species. These terms indicate the total Gibbs free energy of the reaction products and reactants respectfully per mole of Al reacted[2]. If the reaction was set to occur in standard temperature and pressure conditions ($T = 273K$ and $P = 1atm$), standard formation free energies could be used for each of the specific free energy terms; however, changing the operating temperature and pressure conditions makes this a more complicated task.

2.2 Adapting Model to Real Conditions

To understand how the favorability of each aluminum-water reaction byproduct changes as a function of operating temperature and pressure conditions, relationships must first be established to understand how free energy, enthalpy, and entropy change with temperature and pressure. This must be applied to specific free energy, specific enthalpy and specific entropy to determine how temperature and pressure affects each chemical component in the reaction independently. Equations 2.5 - 2.7 represent the dependence of these five variables on each other.

$$dg = dh - Tds - sdT \tag{2.5}$$

$$dh = Tds + vdP \tag{2.6}$$

$$ds = (\frac{\delta s}{\delta T}|_P)dT + (\frac{\delta s}{\delta P}|_T)dP \tag{2.7}$$

Using the definition of specific heat capacity (2.8) and implementing Maxwell's equations to transform $\frac{\delta s}{\delta T}|_P$ (2.9), equation 2.7 can be rearranged to equation 2.10 for the

[2]Enthalpy H and entropy S can be broken down into specific enthalpies and specific entropies in the same way

incremental change in specific entropy.

$$c_P = T(\frac{\delta s}{\delta T}|_P) \tag{2.8}$$

$$\frac{\delta s}{\delta P}|_T = -\frac{\delta v}{\delta T}|_P \tag{2.9}$$

$$ds = \frac{c_P}{T}dT - (\frac{\delta v}{\delta T}|_P)dP \tag{2.10}$$

ds can then be substituted into the dh equation (2.6), resulting in equation 2.11 below. dh and ds can then be substituted into equation 2.5 for dg and simplified from equation 2.12 to equation 2.13.

$$dh = c_P dT + [(v - T(\frac{\delta v}{\delta T}|_P)]dP \tag{2.11}$$

$$dg = c_P dT - sdT + [(v - T(\frac{\delta v}{\delta T}|_P)]dP - T[\frac{c_P}{T}dT - (\frac{\delta v}{\delta T}|_P)]dP \tag{2.12}$$

$$dg = -sdT + vdP \tag{2.13}$$

Now dependent on T and P only, dh and dg can be integrated with respect to both temperature and pressure (2.14 and 2.15). These Δh and Δg terms represent the difference between the specific enthalpy/free energy of a substance at a given operating temperature and pressure and the standard specific enthalpy/free energy of the same substance at standard temperature and pressure (STP).

$$\Delta h = \int_{273K}^{T} c_P dT + \int_{1atm}^{P} [v - T(\frac{\delta v}{\delta T}|_P)]dP \tag{2.14}$$

$$\Delta g = -\int_{273K}^{T} sdT + \int_{1atm}^{P} vdP \tag{2.15}$$

Most specific Gibbs free energy and specific enthalpy data that is available is representative of chemical properties at STP. Δg and Δh can be calculated based on the above equations using non-STP values and used to modify known values and models

to simulate scenarios of interest.

$$\Delta G(T,P) - \Delta G_{STP} = [\Delta g_{Al(OH)_{3(s)}}(T,P) + \frac{3}{2} \cdot \Delta g_{H_{2(g)}}(T,P)] \\ -[\Delta g_{Al_{(s)}}(T,P) + 3 \cdot \Delta g_{H_2O_{(l)}}(T,P)] \quad (2.16)$$

However, the only substance that is affected by changes in operating pressure is H_2 as solids are unaffected and water is incompressible. So equation 2.16 can be reduced to equation 2.17 and the equivalent can be done for enthalpy in equation 2.18.

$$\Delta G(T,P) - \Delta G_{STP} = [\Delta g_{Al(OH)_{3(s)}}(T) + \frac{3}{2} \cdot \Delta g_{H_{2(g)}}(T,P)] \\ -[\Delta g_{Al_{(s)}}(T) + 3 \cdot \Delta g_{H_2O_{(l)}}(T)] \quad (2.17)$$

$$\Delta H(T,P) - \Delta H_{STP} = [\Delta h_{Al(OH)_{3(s)}}(T) + \frac{3}{2} \cdot \Delta h_{H_{2(g)}}(T,P)] \\ -[\Delta h_{Al_{(s)}}(T) + 3 \cdot \Delta h_{H_2O_{(l)}}(T)] \quad (2.18)$$

The equations above represents changes in the ΔG and ΔH of the aluminum hydroxide reaction as T and P deviate from STP conditions assuming that Al, $H_2O_{(l)}$, $Al(OH)_3$ and H_2 are the only substances involved.[3] This is not a sound assumption to make as pre-pressurization requires an inert gas such as nitrogen and the reaction itself is so exothermic that much of the initial water in the system is converted to steam instead of reacting. Further modifications must be made to equation 2.17 before the reaction can be accurately represented.

2.2.1 Factoring in Nitrogen

Although the nitrogen in the reaction setup does not participate in the aluminum-water chemical reaction, it does have a significant effect on the Gibbs free energy calculation. As seen in equation 2.17, hydrogen gas is the only reaction component that is affected by changes in the reaction operating pressure; however, the pressure

[3]The same can be done for $AlOOH$ and Al_2O_3 reactions by applying the respective stoichiometry

that it is dependent on is its partial pressure (PP_{H_2}). In the scenario directly represented by equation 2.17, $PP_{H_2} = P$ because hydrogen is the only gas in the system, but when nitrogen is taken into consideration, it is evident that $PP_{H_2} < P$. The partial pressure of hydrogen is defined as:

$$PP_{H_2} = \frac{N_{H_2}}{N_{tot}} P \tag{2.19}$$

If hydrogen is the only gas in the system, $N_{tot} = N_{H_2}$, but in reality,

$$N_{tot} = N_{H_2} + N_{H_2} + N_{H_2O_{(g)}} \tag{2.20}$$

As the initial system pressure is increased, the number of moles of nitrogen in the system also increases. Nitrogen can be treated as an ideal gas, so the number of moles of nitrogen in the system can be calculated as a function of the operating pressure, operating temperature and system volume as seen in equation 2.21 below.

$$N_{N_2} = \frac{PV}{RT} \tag{2.21}$$

Putting N_{N_2} in terms of variable T and P brings this model one step closer to simulating real conditions.

2.2.2 Factoring in Steam

The last piece of the puzzle required to accurately simulate byproduct favorability of aluminum-water reactions is the steam production ratio. Water that boils off into steam in the reaction chamber does not directly impact the chemical composition of the reactants or products or the reaction stoichiometry; however, it does impact the reaction environment. The steam production ratio (the number of moles of water boiled off for every mole of aluminum reacted) is very important because, similar to nitrogen, it is part of what determines how many moles of gas are in the reaction chamber which in turn affects the partial pressures of all of the gases involved. The main assumption in determining this steam production ratio is that all of the heat

produced by the chemical reaction (ΔH) goes into boiling water, so equations 1.1 - 1.3 can be modified to equations 2.22 - 2.24 below.

$$Al + (3+X)H_2O_{(l)} \rightarrow Al(OH)_3 + \frac{3}{2}H_2 + XH_2O_{(g)} \tag{2.22}$$

$$Al + (2+Y)H_2O_{(l)} \rightarrow AlOOH + \frac{3}{2}H_2 + YH_2O_{(g)} \tag{2.23}$$

$$Al + (\frac{3}{2}+Z)H_2O_{(l)} \rightarrow \frac{1}{2}Al_2O_3 + \frac{3}{2}H_2 + ZH_2O_{(g)} \tag{2.24}$$

Determining coefficients X, Y and Z under the assumption that the heat of the reaction is completely absorbed by the process of boiling water requires balancing the above equations and finding the unknown coefficients for each of the three reactions that produces an overall reaction $\Delta H(T,P)$ of zero. Modifying equation 2.18 with the steam stoichiometry in equation 2.22 yields:

$$\begin{aligned}\Delta H(T,P) = \Delta H_{STP} + [\Delta h_{Al(OH)_{3(s)}}(T) + \frac{3}{2}\cdot\Delta h_{H_{2(g)}}(T, PP_{H_2}) \\ +X\cdot\Delta h_{H_2O_{(g)}}(T, PP_{H_2O_{(g)}})] - [\Delta h_{Al_{(s)}}(T) + (3+X)\cdot\Delta h_{H_2O_{(l)}}(T)]\end{aligned} \tag{2.25}$$

In addition to being dependent on T and/or P, Δh (defined in equation 2.14) is dependent on c_P, v and $\frac{\delta v}{\delta T}|_P$. These are all substance-specific properties, and in the case of water, these properties can not be accurately represented by equations. Therefore, determining coefficient X requires iterative simulation[4].

2.2.3 Final Modeling Method

Taking all of these chemical equations into account, a simulation was constructed in MATLAB. The code took two user inputs: the volume of the reaction chamber setup and the mass of aluminum being reacted. From those two values, the number of moles of nitrogen present in the system at the start of the reaction could be determined (following equation 2.21) for any pressure as well as the number of moles of hydrogen produced over the course of the entire reaction (following stoichiometry and assuming

[4]Finding Y and Z can be done using the same method but applying the respective stoichiometry

the reaction reacted to completion). These values were calculated and input into a simulation which determined the number of moles of steam that would be produced (X, Y and Z) per mole of aluminum reacted in the case that $Al(OH)_3$, $AlOOH$ or Al_2O_3 was produced in various temperature and pressure conditions, following the method described in equation 2.25.

Change in enthalpy of the reaction as a function of temperature only was determined using equations provided by the MIT Department of Materials Science and Engineering. These equations, listed explicitly in Appendix B, yield $\Delta H(T)_{stoich}$ for the aluminum-water reaction at any temperature of interest without taking into account water that is boiled off in to steam. This equation can be represented by equation 2.26 below.

$$\Delta H(T)_{stoich} = \Delta H_{STP} + [\Delta h_{Al(OH)_{3(s)}}(T) + \frac{3}{2} \cdot \Delta h_{H_{2(g)}}(T) - [\Delta h_{Al_{(s)}}(T) + 3 \cdot \Delta h_{H_2O_{(l)}}(T)] \quad (2.26)$$

The following modifications were made to the $\Delta H(T)_{stoich}$ equation provided by MIT DMSE to take into account the dependence on pressure and the use of produced heat to boil off extra water in the system.

$$\Delta H(T,P)_{actual} = \Delta H(T)_{stoich} + X \cdot H_{H_2O_{(g)}}(T) - X \cdot H_{H_2O_{(l)}}(T) + [\frac{3}{2} \cdot \Delta h_{H_{2(g)}}(PP_{H_2}) + X \cdot \Delta h_{H_2O_{(g)}}(PP_{H_2O_{(g)}})] \quad (2.27)$$

Based on equation 2.14, the Δh terms in equation 2.27 can be expanded into terms of specific volume, temperature, and partial pressure as seen below in equations 2.28 and 2.29.

$$\Delta h_{H_2}(PP_{H_2}) = \int_{1atm}^{PP_{H_2}} [v_{H_2} - T(\frac{\delta v_{H_2}}{\delta T}|_P)]dPP_{H_2} \quad (2.28)$$

$$\Delta h_{H_2O_{(g)}}(PP_{H_2O_{(g)}}) = \int_{1atm}^{PP_{H_2O_{(g)}}} [v_{H_2O_{(g)}} - T(\frac{\delta v_{H_2O_{(g)}}}{\delta T}|_P)]dPP_{H_2O_{(g)}} \quad (2.29)$$

Using these expanded equations in addition to the known enthalpy values for

water and steam as a function of temperature at atmospheric pressure, the coefficients X, Y and Z were determined, allowing the partial pressure of hydrogen gas in the system to be accurately calculated for each respective byproduct at various operating temperatures and pressures. With this value determined, the ΔG of each scenario could then be calculated to determine the favorability of each reaction. From equation 2.17 we know that the following is true:

$$\Delta G(T,P) = \Delta G_{STP} + [\Delta g_{Al(OH)_{3(s)}}(T) + \frac{3}{2} \cdot \Delta g_{H_{2(g)}}(T, PP_{H_2})] \\ -[\Delta g_{Al_{(s)}}(T) + 3 \cdot \Delta g_{H_2O_{(l)}}(T)] \tag{2.30}$$

Again, change in gibbs free energy of the reaction as a function of temperature only was determined using equations provided by MIT DMSE. The explicit equations are listed in Appendix C, but can be represented by equation 2.31 below.

$$\Delta G(T)_{stoich} = \Delta G_{STP} + [\Delta g_{Al(OH)_{3(s)}}(T) + \frac{3}{2} \cdot \Delta g_{H_{2(g)}}(T)] \\ -[\Delta g_{Al_{(s)}}(T) + 3 \cdot \Delta g_{H_2O_{(l)}}(T)] \tag{2.31}$$

Combining equation 2.30 and equation 2.31 yields the ΔG value as a function of various operating temperatures and pressures for the actual system:

$$\Delta G(T,P)_{actual} = \Delta G(T)_{stoich} + \frac{3}{2} \cdot \Delta g_{H_{2(g)}}(PP_{H_2}) \tag{2.32}$$

Expanding $\Delta g_{H_{2(g)}}(PP_{H_2})$ using equation 2.15 above yields equation 2.33, revealing the dependence of the system's favorability on the specific volume and partial pressure of hydrogen[5].

$$\Delta g_{H_2}(PP_{H_2}) = \int_{1atm}^{PP_{H_2}} [v_{H_2} - T(\frac{\delta v_{H_2}}{\delta T}|_P)] dPP_{H_2} \tag{2.33}$$

[5]Please note that all of the equations in this subsection focus on finding the change in Gibbs free energy for the $Al(OH)_3$ reaction, but the same method can be applied to the $AlOOH$ and Al_2O3 reactions by applying the respective stoichiometry.

2.3 Modeling Results and Conclusion

This simulation was completed by modeling a situation in which $5g$ of aluminum is reacted with water in a reaction chamber that has a volume of $200mL$. Figures 2-1 through 2-3 below show the results of this simulation at three different operating pressures: $101.3kPa$ (atmospheric pressure), $550kPa$ and $3000kPa$. The byproduct with the most negative ΔG value at each temperature is the byproduct that is most favorable at that temperature and pressure. These three graphs give a sense of how the profile of ΔG values and crossover temperatures change as the pressure of the system increases. The summary of the crossover points can be found in Table 2.1.

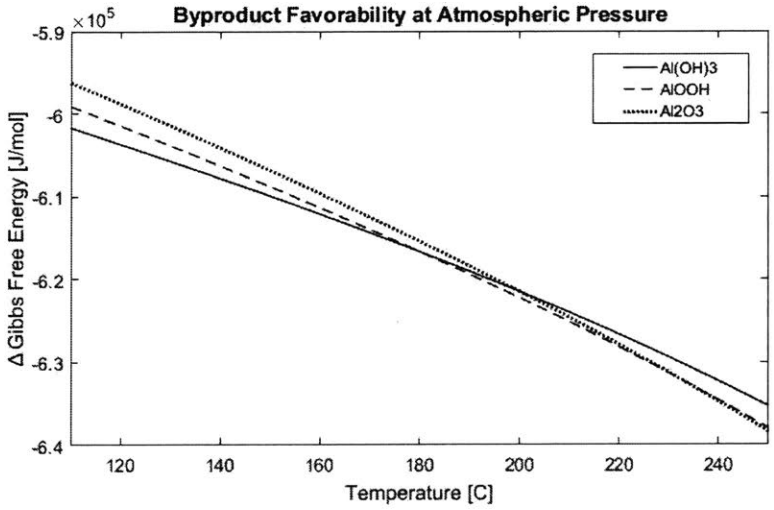

Figure 2-1: Simulated ΔG favorability for each of the three aluminum-water reactions as a function of temperature at atmospheric pressure

The simulation reveals the temperatures and pressures at which we can expect to see a transition in the reaction byproduct; however, one major detail that needs to be considered is the practicality of the reaction conditions. All three of these chemical reactions require liquid water, and the presence of liquid water in these systems is limited by the boiling point at each respective operating pressure.

The boiling point of water at each of the three operating pressures represented in Figures 2-1 through 2-3 is listed in the fourth column of Table 2.1 which gives a sense of what byproduct is actually achievable at each of the three operation pressures. At

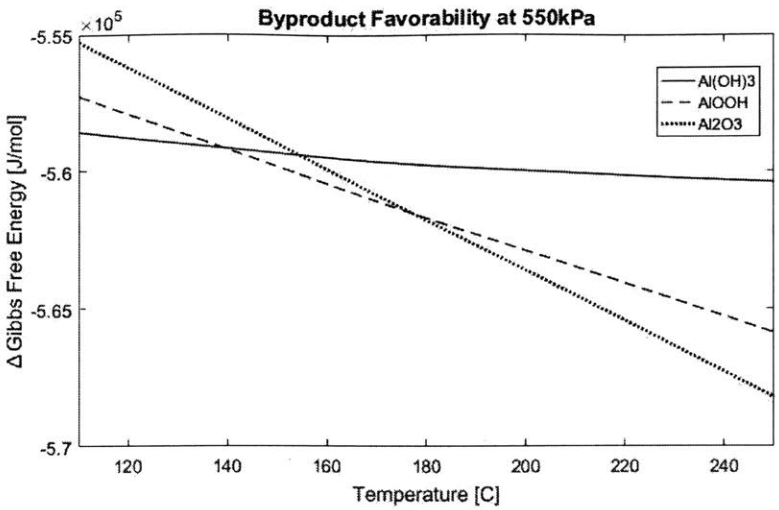

Figure 2-2: Simulated ΔG favorability for each of the three aluminum-water reactions as a function of temperature at operating pressure $550kPa$

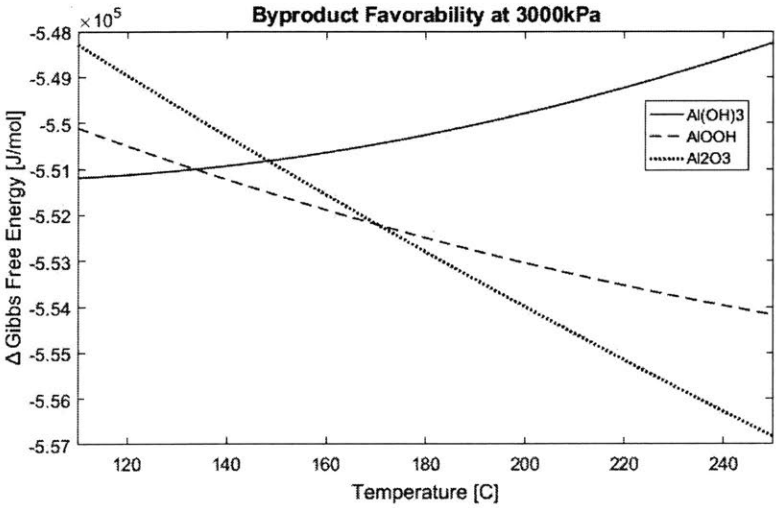

Figure 2-3: Simulated ΔG favorability for each of the three aluminum-water reactions as a function of temperature at operating pressure $3000kPa$

atmospheric pressure, we do not expect to see any byproduct other than $Al(OH)_3$ as the required temperatures to transition to either $AlOOH$ or Al_2O_3 are well above the atmospheric boiling point of water. At $550kPa$, we would only be able to produce $Al(OH)_3$ or $AlOOH$ and at $3000kPa$ we would be able to any of the three byproducts depending on the operating temperature.

To fully understand the achievability of each byproduct as a function of the reac-

Pressure	$Al(OH)_3$ to $AlOOH$	$AlOOH$ to Al_2O_3	Boiling Point
$101.3kPa$	$180°C$	$232°C$	$100°C$
$550kPa$	$139°C$	$177°C$	$156°C$
$3000kPa$	$133°C$	$170°C$	$235°C$

Table 2.1: Temperatures at which $AlOOH$ becomes more favorable than $Al(OH)_3$ and at which Al_2O_3 becomes more favorable than $AlOOH$ at different pressure conditions compared to the boiling point of water at that pressure

tion operating conditions, the favorability crossover points were plotted as a function of temperature and pressure alongside the boiling point of water as a function of pressure in Figure 2-4.

Modeling the change in Gibbs free energy for each chemical reaction at operating temperatures varying from $100°C$ to $300°C$ and operating pressures varying from atmospheric pressure ($101.3kPa$) to $8600kPa$ yielded results that conflicted with the original prediction made by the Department of Energy concerning the crossover in favorability between the three aluminum-water reaction byproducts. The DOE predicted that $AlOOH$ would become more favorable than $Al(OH)_3$ at $280°C$ and Al_2O_3 would become more favorable than $AlOOH$ at $480°C$. This simulation, however, revealed that for a system with a reactor chamber volume of $200mL$ in which $5g$ of aluminum are reacted with water, $AlOOH$ actually becomes favorable over $Al(OH)_3$ at $142.38°C$ and $387kPa$ and Al_2O_3 becomes favorable over $AlOOH$ at $174.21°C$ and $889kPa$. These results are shown below in Figure 2-4.

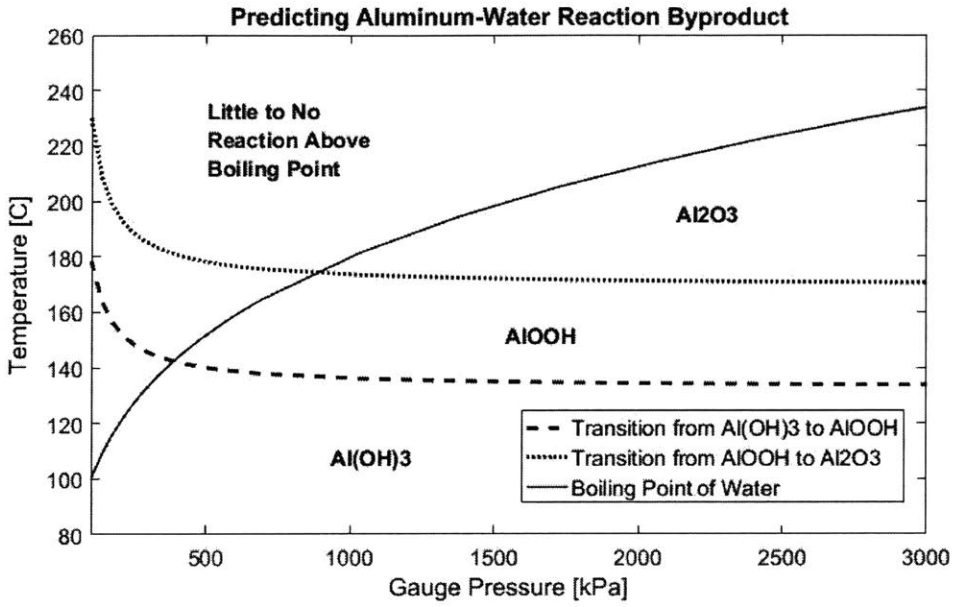

Figure 2-4: Graph of simulated byproduct transition conditions

Chapter 3

Pressurized Testing

As previously mentioned and depicted in equations 1.1 - 1.3, manipulating aluminum-water reactions to produce an oxidized aluminum species that carries fewer hydrogen atoms allows the reaction to consume less water per mole of hydrogen gas that is produced and fed into a hydrogen fuel cell. As explained in Chapter 2, this can be achieved by altering the reaction operating conditions of temperature and pressure. This is the experimental portion of this thesis and will discuss how the changes in those reaction conditions were implemented along with the results of those tests.

3.1 Test Objectives

The main goal of these experiments was to control the temperature of aluminum-water reactions to determine a point at which the byproduct of these reactions switches from $Al(OH)_3$ to $AlOOH$. The gallium-treated aluminum fuel being used reacts readily with liquid water, and maintaining H_2O in liquid form[1] while elevating the reaction temperature requires an accompanying increase in system pressure. The critical point of water is $647K$ or $374°C$ and $22.064MPa$ which is a physical limitation that restricts the reaction from occurring in conditions more extreme than these, as liquid water will not exist in those cases and the reaction will be unable to proceed.

[1]This fuel also reacts with steam; however, it is clear that the aluminum-steam reaction takes place much less readily and further testing is still require to understand it.

Although it was determined through the simulation described in Chapter 2 that $AlOOH$ should become favorable over $Al(OH)_3$ at $142.38°C$ and $387kPa$ and Al_2O_3 should become favorable over $AlOOH$ at $174.21°C$ and $889kPa$, these tests were initially designed to verify the Department of Energy's study, visualized in Figure 1-7, which indicates that $Al(OH)_3$ is the favorable form between room temperature and $280°C$, $AlOOH$ is the favorable form between $280°C$ and $480°C$, and Al_2O_3 is the favorable form at reaction temperatures above $480°C$ [6, 12]. Under these original assumptions, Al_2O_3 is not a viable byproduct of aluminum-water reactions as the temperature of $480°C$ required to switch byproducts from $AlOOH$ to Al_2O_3 is well above the critical point of water. With this in mind, testing was designed specifically to produce $AlOOH$ by exceeding temperatures of $280°C$. The main objective, then, was to react aluminum with liquid water at temperatures up to $300°C$ with corresponding pressures up to $8600kPa$. Considering the extreme exothermic nature of the reaction, the pressure was the only condition set by the user and the heat of the reaction was used to increase the temperature of the setup to the boiling point of water at that pressure.

3.2 Testing Setup

3.2.1 Functional Requirements & Design Considerations

Based on the fact that this reaction entails combining gallium-treated aluminum spheres with liquid water to produce potentially dangerous hydrogen gas in a high pressure and high temperature environment, the following functional requirements listed in Table 3.1 were established for the test setup to ensure reliable and safe practice.

Requirements 1 and 2 were derived directly from the test objectives for varying the reaction conditions. Requirements 3 and 4 take into consideration material compatibility for the chemicals involved in the reaction. While there are no compatibility risks for aluminum and its oxidized species, there are risks of both hydrogen and

	Requirement	Specification
1	Temperature Threshold	withstand $> 300°C$
2	Pressure Threshold	withstand $> 8600kPa$
3	Gallium Embrittlement	all materials used must be known to show negligible to no susceptibility
4	Hydrogen Embrittlement	all materials used must be known to show negligible to no susceptibility
5	Water Compatibility	all materials must sufficiently resist oxidation by water
6	Reaction Initiation	reactants must be combined only after system has been fully closed and pressurized; combination must be initiated remotely
7	Monitoring	temperature and pressure must be monitored at all times
8	Failsafe	pressure relief valve must be able to be overridden remotely

Table 3.1: Functional Requirement Specifications

gallium penetrating the interior surfaces of the reactor setup and compromising their integrity [4, 20]. Along the same lines, requirement 5 was established to ensure that the water involved in the reaction would not compromise the integrity of the setup by allowing parts to rust and corrode.

Requirements 6, 7 and 8 were put into place for safety purposes. Although it is assumed that the temperature of the reaction will never exceed the boiling point of water at the given operating pressure due to the fact that the exothermic reaction cannot proceed if all of the water boils off, nothing can accurately be predicted as little testing has actually been completed on aluminum-water reactions and there is minimal documentation on these reactions at this scale. Furthermore, the gallium-indium eutectic that is used to treat the aluminum fuel pellets being used in these tests is a novel substance to these reactions, and although its presence is minimal, it is unknown how exactly the eutectic affects the properties of the reaction, nevermind how it might affect the properties of the reaction at elevated temperatures and pressures. Given

all of these unknowns, it is safest to require that the reaction be initiated, completed, and brought back down to room temperature and pressure while the person running the experiment is out of the proximity of the reaction. Remote monitoring was consequently required to indicate to the test supervisor when the temperature and pressure has settled and, in the case that something unexpected happens, when the reaction is getting out of hand and emergency termination is necessary.

3.2.2 System Design

Based on the functional requirements listed in Table 3.1, a robust testing setup was designed and constructed (Figure 3-1).

Figure 3-1: Full test system setup

The system consisted mainly of 316 stainless steel tubing and Swagelok tube fittings. 316 stainless steel was chosen for its resistance to gallium and hydrogen embrittlement and water corrosion. A 1 inch outer diameter tube acted as a reaction chamber, and $\frac{1}{2}$ inch tubes were used to connect the reaction chamber to variety of components via a 4-connector cross fitting (depicted more clearly in Figure 3-2). This modular-style setup was chosen because the Swagelok fittings, which are most ideal

for sealing hydrogen in high temperature and high pressure environments, physically deform the tubes that they are attached to, rendering tubes that require disconnection between tests unusable after one test run. Creating a modular setup reduced the cost of parts for each experiment.

The first of the components connected to the cross connector on the reaction chamber tube was a pressure transducer that was wired to a microcontroller. This allowed the person running the experiment to monitor the setup pressure in real time. To prevent the transducer from overheating, the $\frac{1}{2}$ inch tubing that it was connected to was lined with high temperature mineral wool insulation which was held in place by stainless steel mesh.

The second component connected to the cross connector was a ball valve leading to the nitrogen tank used to pre-pressurize the system. The ball valve acted as a second layer of protection in addition to the pressure regulator to ensure that hydrogen gas did not make its way from the reaction setup into the tank. Nitrogen tanks are susceptible to hydrogen embrittlement, so extra caution was taken to make sure that the integrity of the tank would not be compromised.

The third component attached to the cross connector was the fuel feeder. This feeder consisted of a $\frac{1}{2}$ inch tube lined with a PTFE tube to reduce the inner diameter to prevent fuel pellet jamming. Prior to the start of the reaction, a valve connecting the feeder tube to the cross connector prevented the fuel from prematurely falling into the reaction chamber tube below. Mounted above the feeder tube was a relief valve which could be calibrated to maintain the desired pressure inside of the setup. A piece of 316 stainless steel mesh was was inserted at the connection between the feeder tube and the regulator to prevent fuel pellets from jamming and blocking the relief valve.

Although not pictured, the reaction chamber tubing was placed inside of a bucket of high temperature mineral wool insulation during testing. Thermocouples were attached to the outside of the base of the reaction tube and connected to the same microcontroller as the pressure transducer, enabling remote temperature monitoring. The insulation was used so that the thermocouples on the exterior of the tubing would

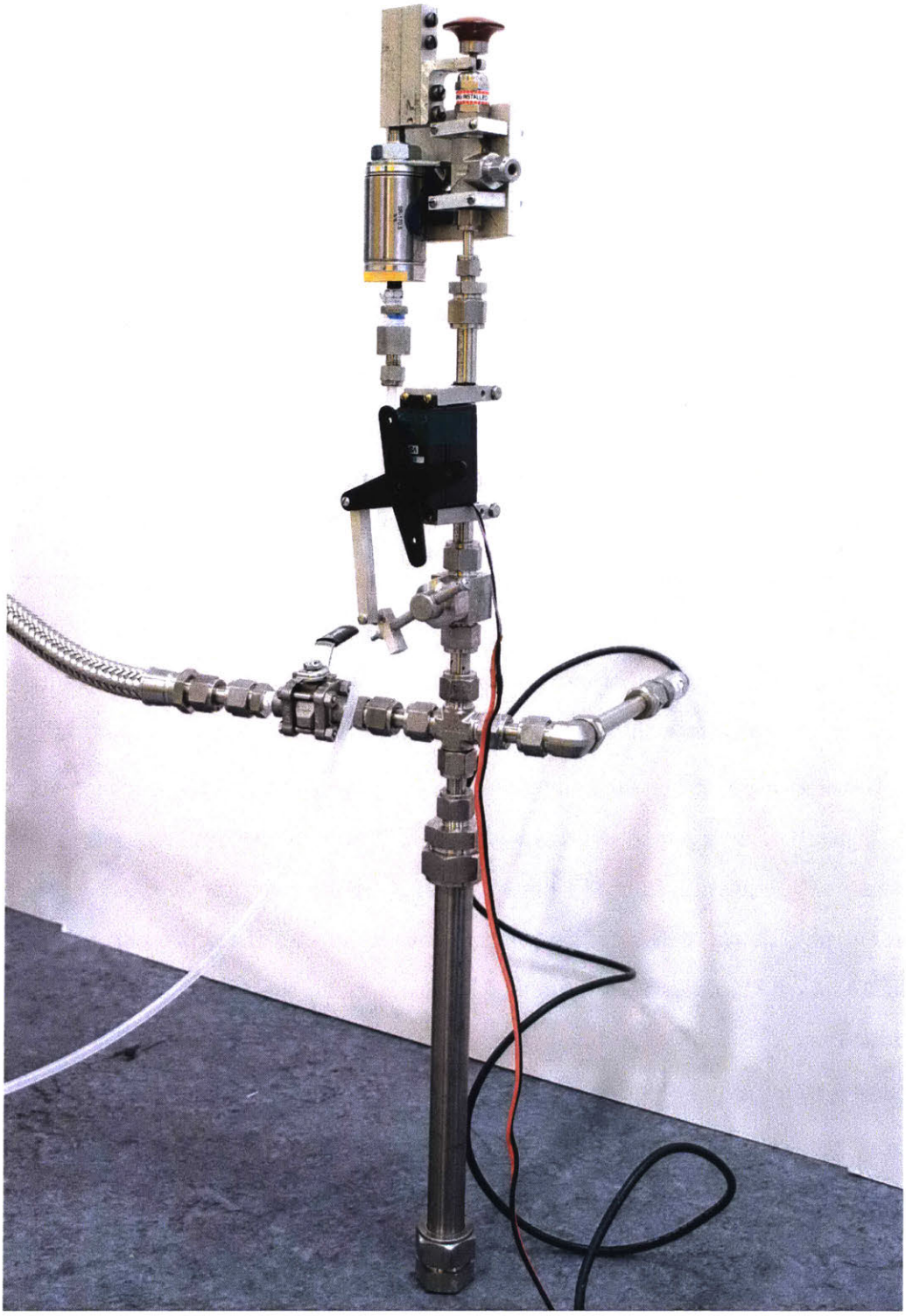

Figure 3-2: Main body of the test setup

read out temperatures that were as close as possible to the temperature of the interior of the tube. Running thermocouples into the interior of the setup posed the risk of significant pressure leakage, so they remained outside of the reaction.

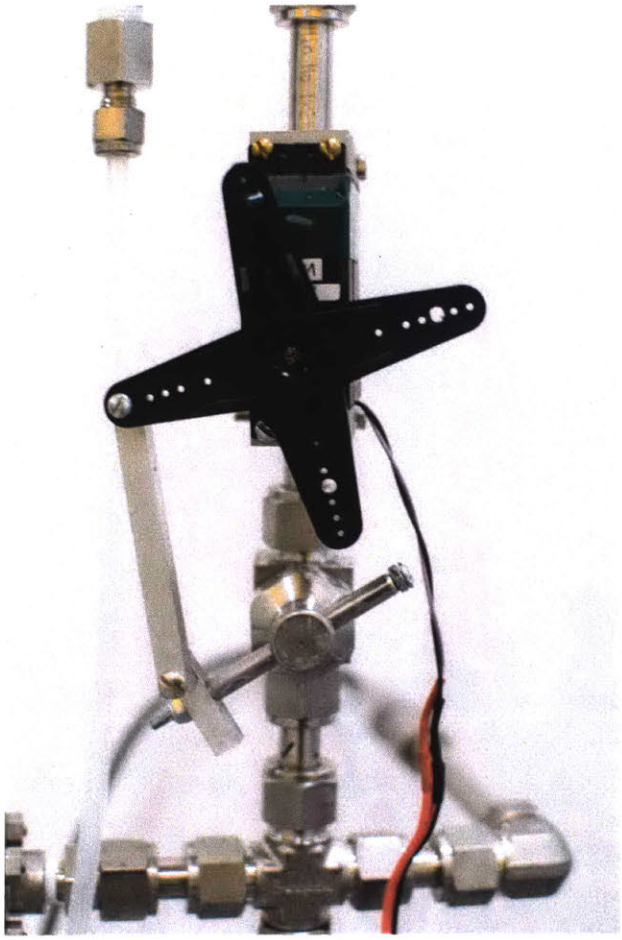

Figure 3-3: 4-bar mechanism initiation actuator

Meeting functional requirements 6 and 8 in Table 3.1 required two actuators: a motor-driven 4-bar linkage and a pneumatic cylinder, pictured in Figures 3-3 and 3-4 respectively. The motorized 4-bar linkage was attached to the feeder tube and coupled to the valve which blocked or allowed the aluminum fuel pellet to fall into the reaction chamber below. The pneumatic cylinder was mounted to a plate that was constrained to the relief valve. The bore was coupled to a custom piece which rested under the valve's manual relief handle. When air was allowed to flow into the cylinder, the bore would pop up, forcing the handle upwards, opening the relief valve and allowing the setup to return to atmospheric pressure.

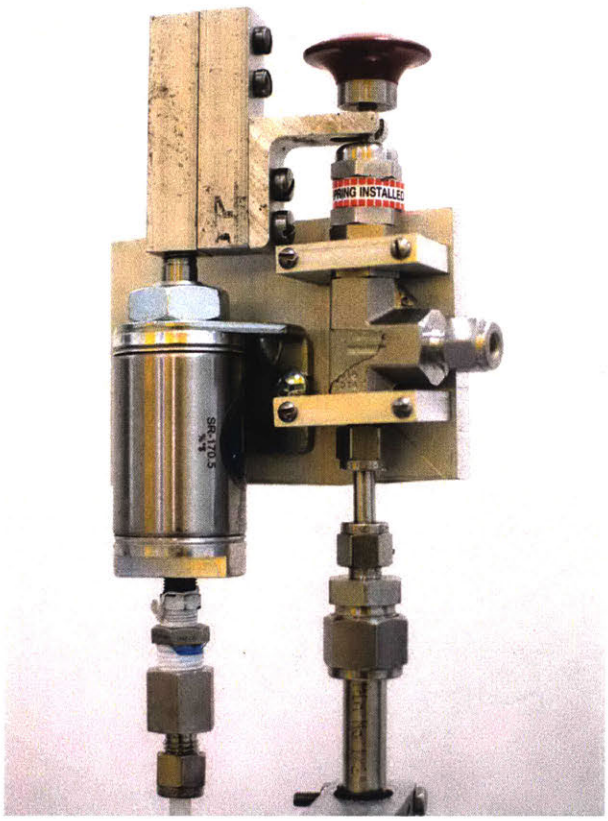

Figure 3-4: Relief valve and pressure fail-safe

Due to the risk of a high pressure burst in the setup, this setup was designed to be operated from a distance of about $30ft$ with the base of the chamber (where the highest temperatures were expected) surrounded by a barrier of cinder blocks to prevent shrapnel from reaching the operator in the case that something unexpected happened. It is known that the rate of aluminum-water reactions increases as the temperature increases, and seeing that these reactions are highly exothermic, the extra precaution was necessary because the operating temperature and pressure can change very rapidly once the reaction commences [19]. Distance was also required because the release of hydrogen gas from high pressures ($>3500kPa$) into an environment of atmospheric pressure poses the risk of autoignition of that gas [25].

After evaluating testing locations around MIT, it was determined that the aerospace engineering blast chamber was the safest and most convenient place for testing,

so the cinder block barrier and large experiment radius were not necessary during actual testing.

3.3 Testing Process

3.3.1 Fuel Preparation

Fuel for these tests was prepared using Jonathon Slocum's recommended heat treatment process [22]. $59.95g$ of aluminum bb pellets were baked in glassware filled with $300g$ of gallium-indium eutectic at $120°C$ for 2 hours and stirred every 30 minutes. After treatment, the fuel was sent through a centrifuge to remove and recover excess eutectic, resulting in $61.24g$ of prepared fuel.

3.3.2 Reaction

Each experiment used $5g$ of the prepared fuel and $30mL$ of water. Setting up the experiment required first pouring the water into the 1 inch reaction chamber tube and attaching that tube to the rest of the setup with Swagelok connectors[2]. The empty $\frac{1}{2}$ inch feeder tube[3] was then attached to the valve above the cross connector. The valve was closed about 90% of the way to prevent fuel from passing through the valve but allowing air to flow freely throughout the entire system. The aluminum bb pellets were then poured into the feeder tube and the entire setup was sealed off with the relief valve on the top. This relief valve was calibrated with each test to ensure that the appropriate pressure would be maintained within the system throughout testing. A model of the closed setup is visualized in Figure 3-5, and Figure 3-6 shows a cross section schematic of the closed system, depicting the reactant setup inside.

Once everything was sealed inside, the system was planted into the insulation and the nitrogen tank, ball valve and pressure regulator were all opened (in that order) to allow nitrogen to pass into the system. The pressure was monitored on a computer through the connected pressure transducer and microcontroller. When the desired

[2]This tube was one of the tubes that was replaced with every test

[3]This component was also replaced with every test

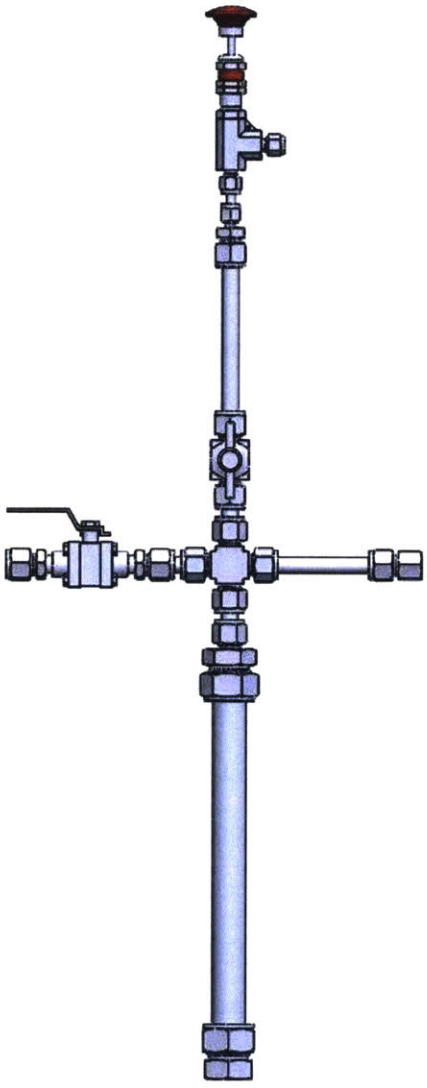

Figure 3-5: Reaction setup model

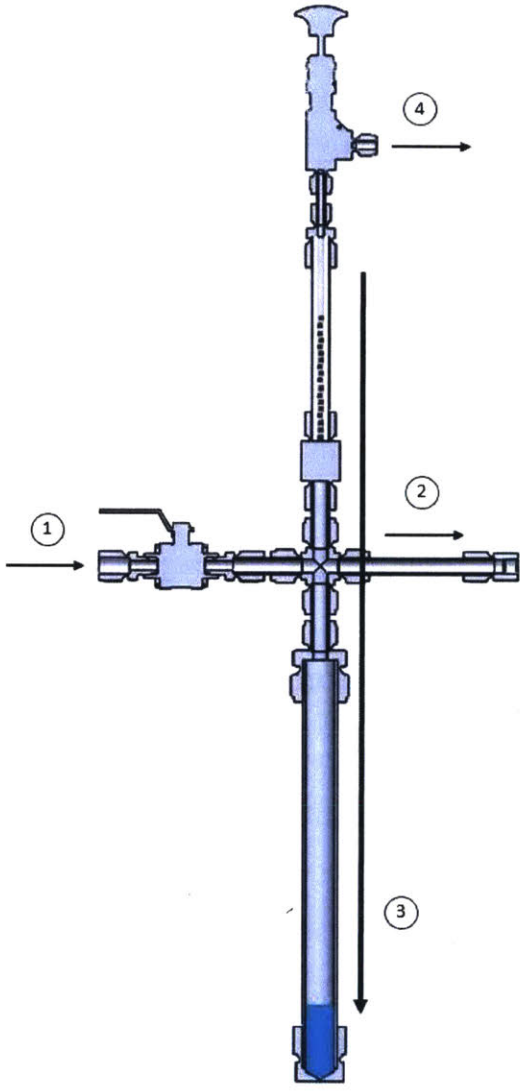

Figure 3-6: Reaction setup cross-section:
1) nitrogen pre-pressurizes the setup
2) pressure transducer detects the pressure
3) fuel drops into water below
4) relief valve expels nitrogen, steam and hydrogen

reaction pressure was achieved, the all three components were closed back up and the blast chamber was evacuated.

From the outside of the blast chamber, the motorized 4-bar linkage was activated and the fuel dropped into the reaction chamber tube below, combining with the water

and commencing the reaction. Pressure and temperature were monitored throughout the process. As the reaction proceeded, the produced hydrogen gas and steam increased the system pressure, activating the relief valve which closed back up once the pressure returned to the set pressure.

The reaction was deemed complete once the temperature of the system had clearly stabilized and started to steadily decline. At this point the relief valve was opened to release pressure and eliminate risk of the system bursting so the experiment operator could reenter the blast chamber and disassemble the tubing to observe the results.

In the case that the relief valve did not properly activate on its own, the operator was able to open the valve on a second nitrogen tank housed outside of the chamber which was attached to the pneumatic fail safe. Introducing pressure to the pneumatic cylinder forced the relief valve open, releasing pressure and preventing both pressure and temperature from climbing to questionably safe values.

These tests were carried out at pressures of $1035kPa$, $1725kPa$, $3450kPa$, $5170kPa$ and $6900kPa$.

3.4 Results

Although testing was not perfect, the results of these high pressure tests proved very successful. The production of $AlOOH$ was detected at pressures as low as $1035kPa$, which corresponds to a boiling point of water of $181°C$. There was, however, no indication that the further dehydrated reaction byproduct Al_2O_3 formed in any of the tests. Images of the oxidized aluminum byproducts can be found below in Figure 3-7.

To better explain what occurred during each experiment to produce the results documented below, refer to Table 3.2 for a list of notes which document the variations between each of the reactions and how the slight deviations from the intended procedure might have affected the outcome.

Figure 3-7: Images of oxidized aluminum byproducts from testing. Top row, left to right: atmospheric pressure, $1035kPa$, $1725kPa$. Bottom Row, left to right: $3450kPa$, $5170kPa$, $6900kPa$

3.4.1 Infrared Spectroscopy

Once testing was complete, samples were extracted, dehydrated and prepared for infrared spectroscopy analysis courtesy of the MIT Materials Science and Engineering Department. The results from this testing are displayed below in Figure 3-9. The resulting spectra were compared to an FTIR test that was done on a known $Al(OH)_3$ sample from an aluminum-water reaction completed at atmospheric pressure[4]. This reference plot is shown in Figure 3-8. It is important to notice the large peak in this graph that occurs at wavenumber $3400cm^{-1}$. This peak is known to correspond to the presence of hydroxide (OH) bonds in a chemical which is logical seeing as $Al(OH)_3$ contains three of these hydroxide bonds per molecule.

The results from the FTIR analysis completed on the pressurized testing samples show a similar peak in the $1035kPa$ case, indicating that much of the byproduct was

[4]This composition was verified by comparing to literature FTIR results[13, 24]

Test Pressure	Boiling Temp	Exterior Temp Recorded	Byproduct	Notes
$1035kPa$	$181°C$	$133.25°C$	$Al(OH)_3$, $AlOOH$	pressure quickly jumped to $1500kPa$ because relief valve was jammed, manual override activated, dropping pressure to $200kPa$ for the duration of the test
$1725kPa$	$205°C$	$167.25°C$	$AlOOH$	relief valve was leaking when it should have closed after opening to regulate pressure, pressure was manually increased to counter effects
$3450kPa$	$242°C$	$173.0°C$	$AlOOH$	steady pressure leak in the relief valve (about $350kPa/min$), majority of reaction occurred between $2050 - 2750kPa$
$5170kPa$	$266°C$	$219.0°C$	$AlOOH$	steady pressure leak in the relief valve (about $350kPa/min$), majority of reaction occurred between $4130 - 5170kPa$
$6900kPa$	$285°C$	$159.25°C$	$AlOOH$	relief valve setting higher than intended, manual override necessary to avoid risk of burst, majority of reaction occurred between $4130 - 5510kPa$

Table 3.2: Test specific notes from running the pressurized aluminum-water reactions in the MIT blast chamber

still $Al(OH)_3$, but as the pressure increases, that hydroxide peak at $3400cm^{-1}$ falls and is replaced by the presence of two distinct peaks within the range of $3000 - 3500cm^{-1}$. Chemical research literature verifies (as seen in Figure A-1 in Appendix A) that this is an indication that the number of hydroxide bonds in the byproduct is decreasing as the operating pressure of the experiment generally increases[5] while the number of oxide bonds (O) is increasing, implying a shift from $Al(OH)_3$ to $AlOOH$.

[5]This is not a perfect trend as there were imperfections in testing (described in Table 3.2)

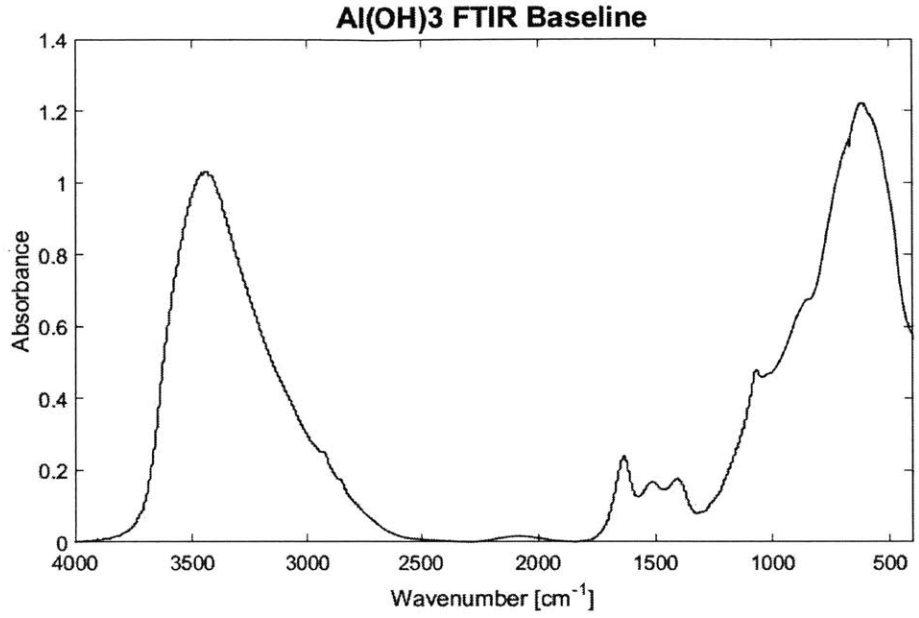

Figure 3-8: FTIR analysis results representing the absorbance spectrum for $Al(OH)_3$ produced by aluminum-water reactions carried out under standard atmospheric conditions

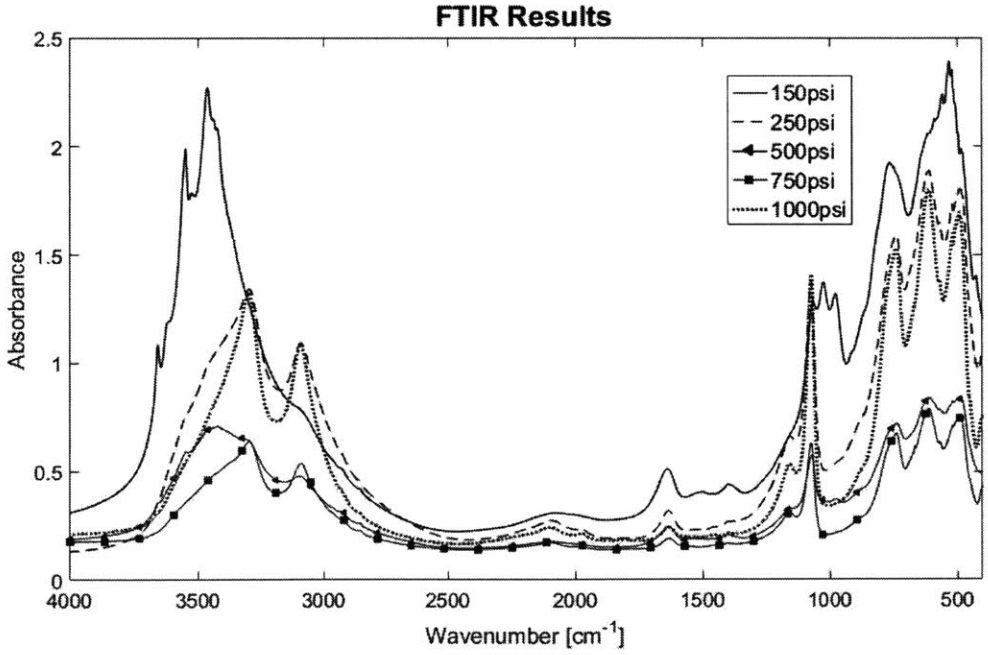

Figure 3-9: FTIR analysis results representing the absorbance spectra of the byproducts of the pressurized aluminum-water reaction tests

3.4.2 X-Ray Diffraction

Running the samples through x-ray diffraction analysis further verified the presence of $AlOOH$ in the pressurized aluminum-water reaction byproduct. The diffraction peaks, seen below in Figures 3-10 through 3-16, were compared against diffraction data found in literature as well as the the material properties database maintained by MIT's Department of Materials Science[2, 18]. Both sources confirmed that the non-$Al(OH)_3$ byproduct that was present was indeed $AlOOH$.

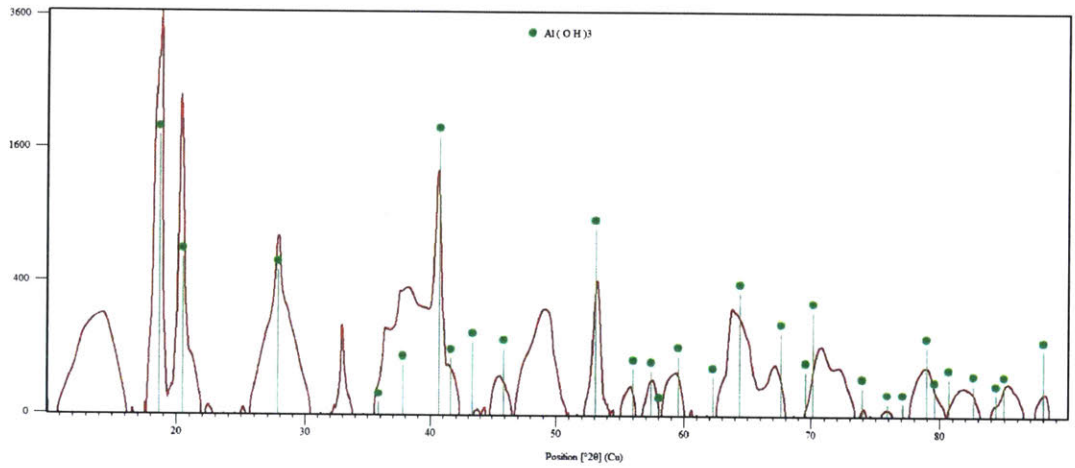

Figure 3-10: X-Ray diffraction peaks from the 1035kPa pressurized aluminum-water reaction compared to known $Al(OH)_3$ diffraction pattern

As seen in Figures 3-10 and 3-11, the majority of the oxidized aluminum species that was present as a byproduct of the $1035kPa$ pressurized reaction was still $Al(OH)_3$. This is likely due the the fact that the majority of the test was run at $200kPa$ (as noted in Table 3.2) due to an error with the relief valve. Regardless, it is still important to note that some amount of $AlOOH$ was produced at pressures as low as $1035kPa$.

The x-ray diffraction analysis of the byproduct of the $1725kPa$ test as seen in Figure 3-12 showed a very strong alignment with the known $AlOOH$ diffraction pattern, indicating that the byproduct was composed almost completely out of $AlOOH$ as opposed to $Al(OH)_3$.

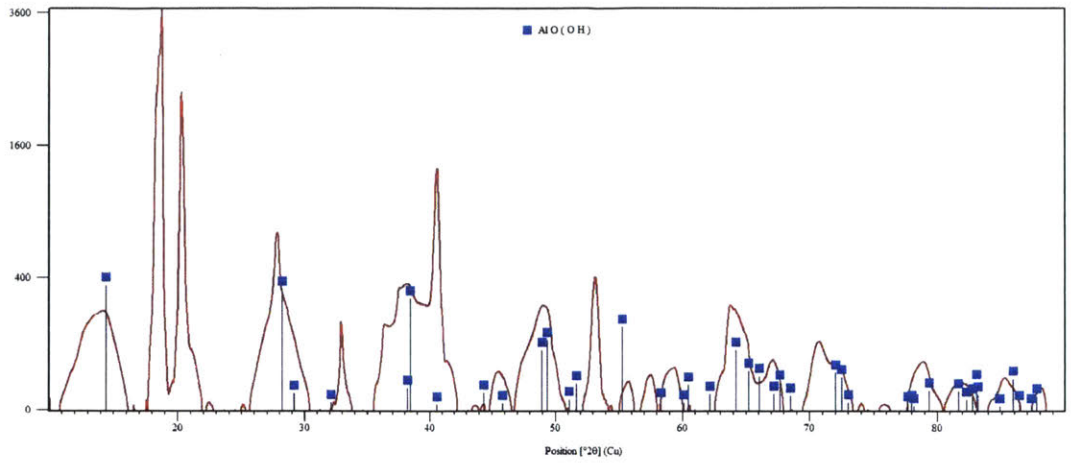

Figure 3-11: X-Ray diffraction peaks from the 1035kPa pressurized aluminum-water reaction compared to known $AlO(OH)$ diffraction pattern

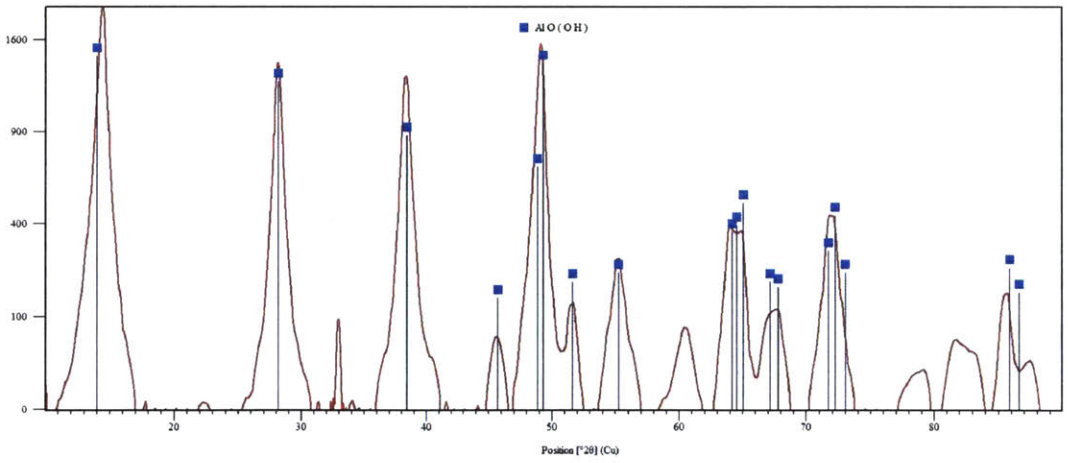

Figure 3-12: X-Ray diffraction peaks from the 1725kPa pressurized aluminum-water reaction compared to known $AlO(OH)$ diffraction pattern

The byproduct from the $3450kPa$ test, on the other hand, produced an x-ray diffraction pattern seen in Figures 3-13 and 3-14 which indicated the presence of both $Al(OH)_3$ and $AlOOH$, but shifted more towards $AlOOH$ than in the $1035kPa$ case. This split is peculiar because, although the leaky pressure relief valve kept the operating pressure on the decline within the setup, the majority of the reaction still took place between $2050kPa$ and $2750kPa$, pressures well above the operating pressure

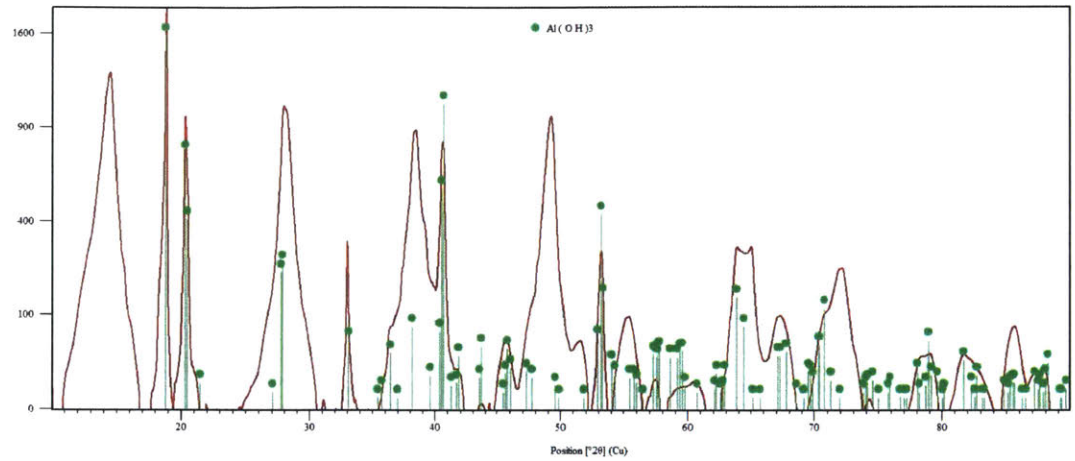

Figure 3-13: X-Ray diffraction peaks from the 3450kPa pressurized aluminum-water reaction compared to known $Al(OH)_3$ diffraction pattern

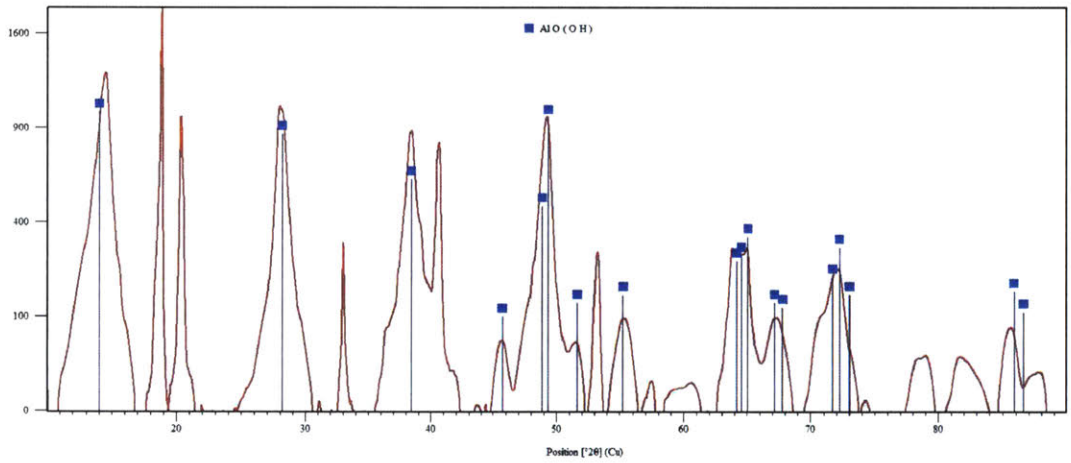

Figure 3-14: X-Ray diffraction peaks from the 3450kPa pressurized aluminum-water reaction compared to known $AlO(OH)$ diffraction pattern

used to produce dominantly $AlOOH$ in the $1725kPa$ test. The relatively low measured temperature of the reaction chamber exterior indicates that it is possible that the reaction was not operating at boiling point; however, the exterior temperature still exceeded the temperature measured in the $1725kPa$ case.

In both the $5170kPa$ and $6900kPa$ cases, a strong alignment was seen between the x-ray diffraction analysis results and the x-ray diffraction pattern that corresponds

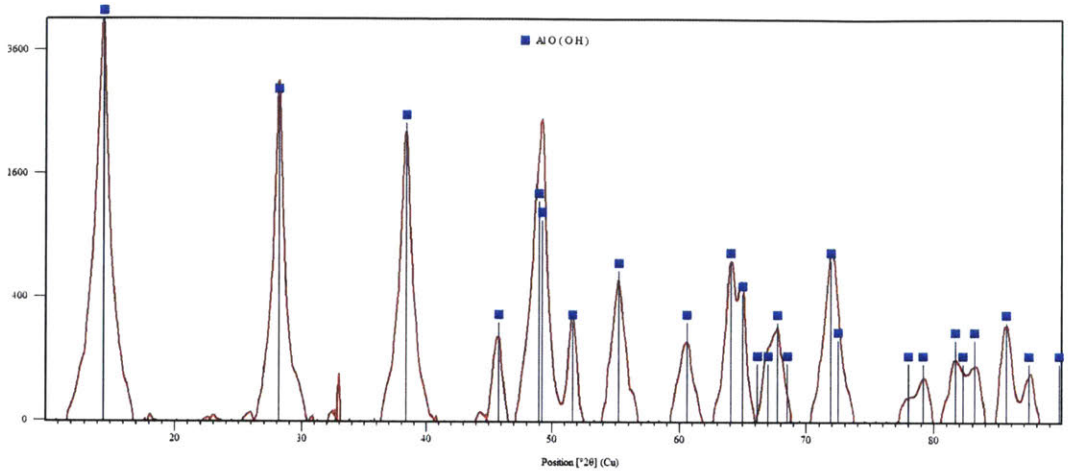

Figure 3-15: X-Ray diffraction peaks from the 5170kPa pressurized aluminum-water reaction compared to known $AlO(OH)$ diffraction pattern

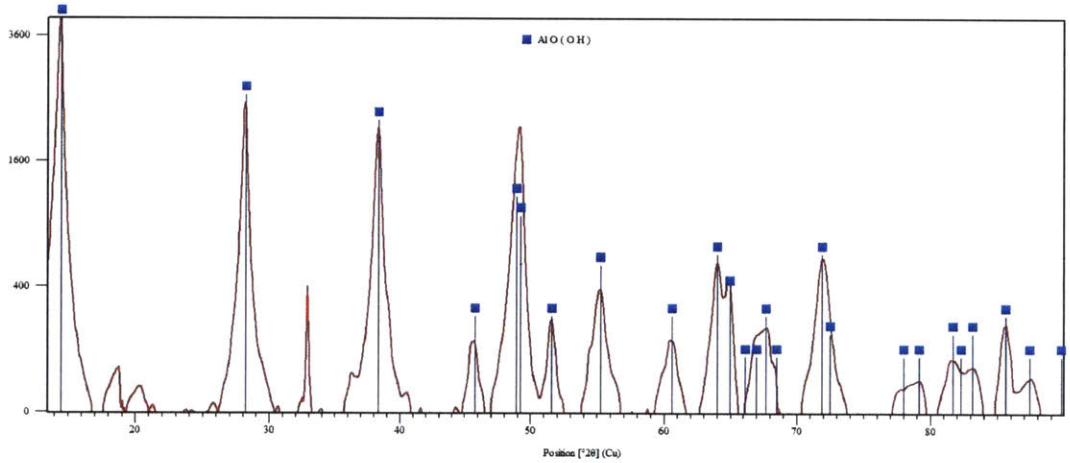

Figure 3-16: X-Ray diffraction peaks from the 6900kPa pressurized aluminum-water reaction compared to known $AlO(OH)$ diffraction pattern

to $AlOOH$, as seen in Figures 3-15 and 3-16, but Al_2O_3 was still not detected in any of the tested byproducts.

3.4.3 Summary

Pressurized aluminum-water reaction tests were carried out using treated aluminum fuel that has been proven an effective fuel for hydrogen production. The byproduct of

the reaction that occurs when water is combined with this fuel at atmospheric pressure was confirmed to be $Al(OH)_3$, the most hydrated of the three byproduct possibilities, but Fourier-transform infrared spectroscopy (FTIR) and x-ray diffraction analysis revealed that, at elevated pressure and temperatures, the same fuel can be used to produce $AlOOH$, a 33% less hydrated byproduct, at pressures as low as $1035kPa$. Simulation predicts that Al_2O_3, a 50% less hydrated byproduct than $Al(OH)_3$, should also have been present as an aluminum-water reaction byproduct within the range of pressures and temperatures that were tested; however, no Al_2O_3 was detected. It is possible, due to the fact that the heat in these tests was produced by the reaction itself, that Al_2O_3 was not see because most or all of the reaction was completed before enough heat was generated to reach the temperature necessary to cause Al_2O_3 to form over $AlOOH$.

THIS PAGE INTENTIONALLY LEFT BLANK

Chapter 4

Discussion and Outlook

4.1 Conclusion

A computational simulation analysis was completed investigating the favorability of the three different byproducts of aluminum-water reactions. By adapting real operating scenario conditions to ideal enthalpy and Gibbs free energy data provided by the MIT Department of Materials Science and Engineering, a comprehensive model was created to calculate temperature and pressure conditions at which aluminum hydroxide ($Al(OH)_3$), aluminum oxy-hydroxide ($AlOOH$) or aluminum oxide (Al_2O_3) becomes favorable over the other two oxidized aluminum byproducts. Applying the parameters of the system that was later tested which reacted $5g$ of gallium-indium treated aluminum fuel with water in a $200mL$ reaction chamber, it was calculated that $AlOOH$ would become favorable over $Al(OH)_3$ at $142.38°C$ and $387kPa$ and Al_2O_3 would become favorable over $AlOOH$ at $174.21°C$ and $889kPa$.

Physical testing was carried out under pressure conditions ranging from $1035kPa$ to $8600kPa$, which allowed the heat of the aluminum-water combination reaction to heat the reaction to temperatures up to the corresponding boiling temperatures at the respective operating pressures ($100°C$ - $300°C$). $AlOOH$ was found to develop at the lowest test pressure of $1035kPa$, which corresponds to a boiling temperature of $181°C$). However, Al_2O_3 was not detected at all during testing, suggesting that there is either a component missing from the simulation or something occurred during the

reactions that prevented the interior of the setup from actually reaching the conditions necessary for Al_2O_3 to become more favorable. Regardless, this thesis proves that it is possible to manipulate the byproducts of hydrogen-generating aluminum-water reactions to consume less water, therefore reducing the amount of reactant required to produce hydrogen and consequently increasing the gravimetric and volumetric energy densities of the system as a whole.

4.2 Future Testing

4.2.1 Testing Improvements

Although the test set up constructed for testing in this thesis maintained testing conditions well enough to show a shift in the aluminum-water reaction byproduct, there are still significant improvements that need to be implemented before the exact byproduct crossover conditions can be experimentally verified. For one, thermocouples need to be integrated into the interior of the reaction chamber so the operating temperature can be more accurately monitored. The relief valve also needs to be replaced by a proper pressure regulator that is capable of maintaining the system pressure within a tighter tolerance of the specified test pressure. The relief valve used here vented and resealed to pressures within only about 15% of the desired operating pressure, allowing for significant fluctuation as the reaction continued to produce hydrogen and steam and build pressure.

In general, these tests would benefit from a more accessible setup and one that can react more than $10g$ of fuel. Due to the fact that all of the aluminum fuel and water are combined at once, the reaction accelerates and becomes violent as the reaction proceeds and temperature rises. To better regulate this reaction, implementing some form of reactant combination control would make this setup simpler while also reducing safety concerns. Furthermore, this would enable control of hydrogen flow out of the system, making it possible to attach the reactor directly to a fuel cell for practical applications.

4.2.2 System Outlook

In order to more clearly understand the aluminum-water reactions at hand, it would be useful to further study the thermodynamics of the system. Aluminum is known to have a significant heat capacity, so one might expect to see superheating of steam at the reaction site where water and aluminum produce heat, hydrogen, and byproduct. Because the reaction releases a significant amount of energy very rapidly and because the aluminum cannot dissipate that heat very quickly, it may be possible that bubbles of superheated steam and hot hydrogen are forming at the reaction sites. This would allow the reaction temperature to rise above the boiling point of water and therefore release the restriction that the reaction temperature used to manipulate the species of byproduct formed is limited by the operating pressure. If this restriction is lifted and the superheat can be quantified, manipulating this hydrogen production reaction may prove much easier than expected.

Also taking into consideration the large amount of steam produced by this reaction and the potential for that steam to be generated at high temperatures near $300°C$, it is possible to couple the system with heat recovery to further increase the energy efficiency of the system. This sort of cogeneration system has already been successfully implemented in a similar system in which molten aluminum is reacted with water, allowing the heat of the reaction to be put to good use, increasing the energy generation efficiency by about 41% - 49% depending on selected turbine configuration [1] [26].

Investigating and implementing these improvements to the aluminum-water reaction hydrogen production system could vastly improve the technology, rendering aluminum fuel both more energy dense and efficient, providing a competitive alternative to fossil fuels for mobile power systems.

[1] Schematics of these heat recovery systems can be seen in Figure A-5.

THIS PAGE INTENTIONALLY LEFT BLANK

Appendix A

Figures

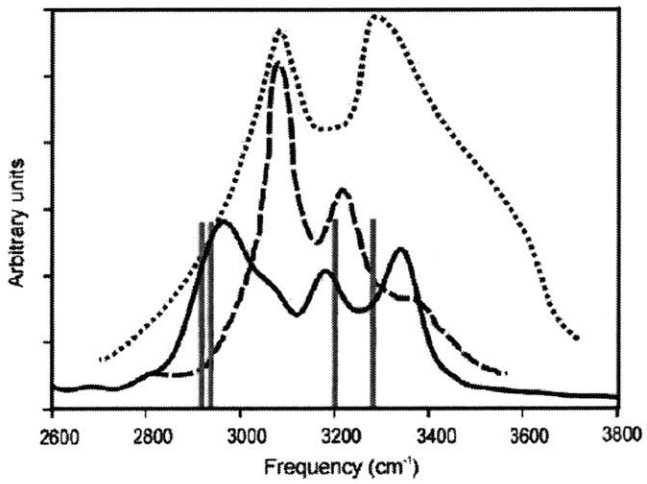

Figure 7. DFT calculated harmonic frequencies of OH stretching modes (vertical gray lines) and corresponding calculated power spectra of hydrogen atoms (solid curve). Dotted and dashed curves are reprinted experimental IR [49] and Raman [50] spectra from the literature.

Figure A-1: Calculated FTIR absorbance spectra for various OH bonds found in aluminum oxyhydroxide crystalline structures [24]

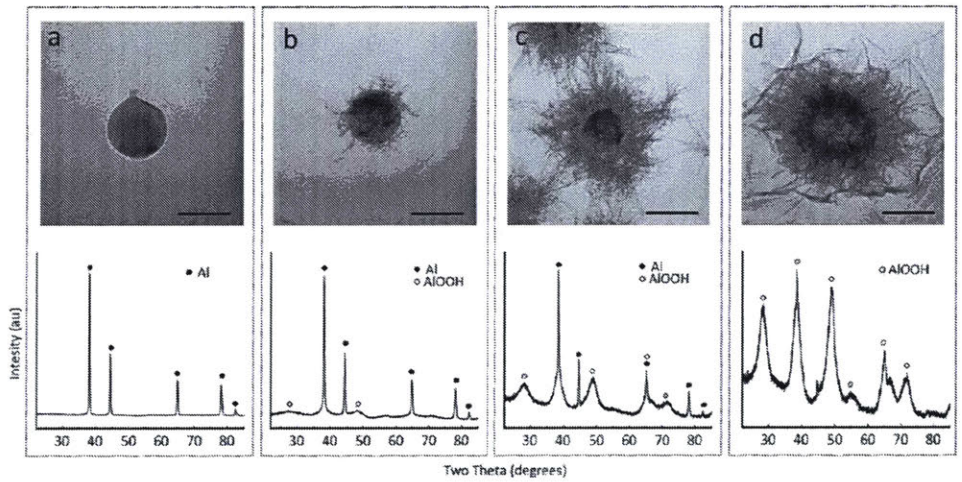

Figure 3. TEM images and XRD patterns of Al nanoparticles at different reaction stages: (a) stage II; (b) stage III; (c) beginning of stage IV; (d) end of stage IV. All bars are 100 nm.

Figure A-2: Documented x-ray diffraction spectra for *AlOOH* [18]

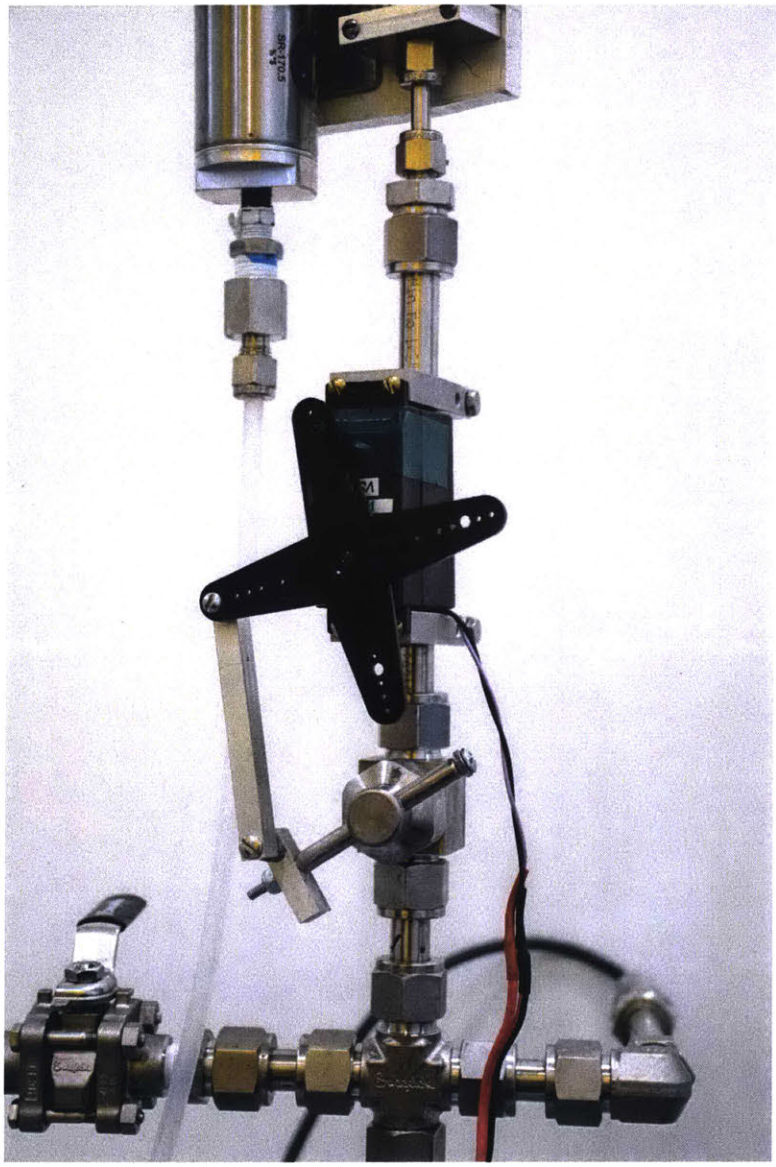

Figure A-3: Close up image of reaction initiation actuator

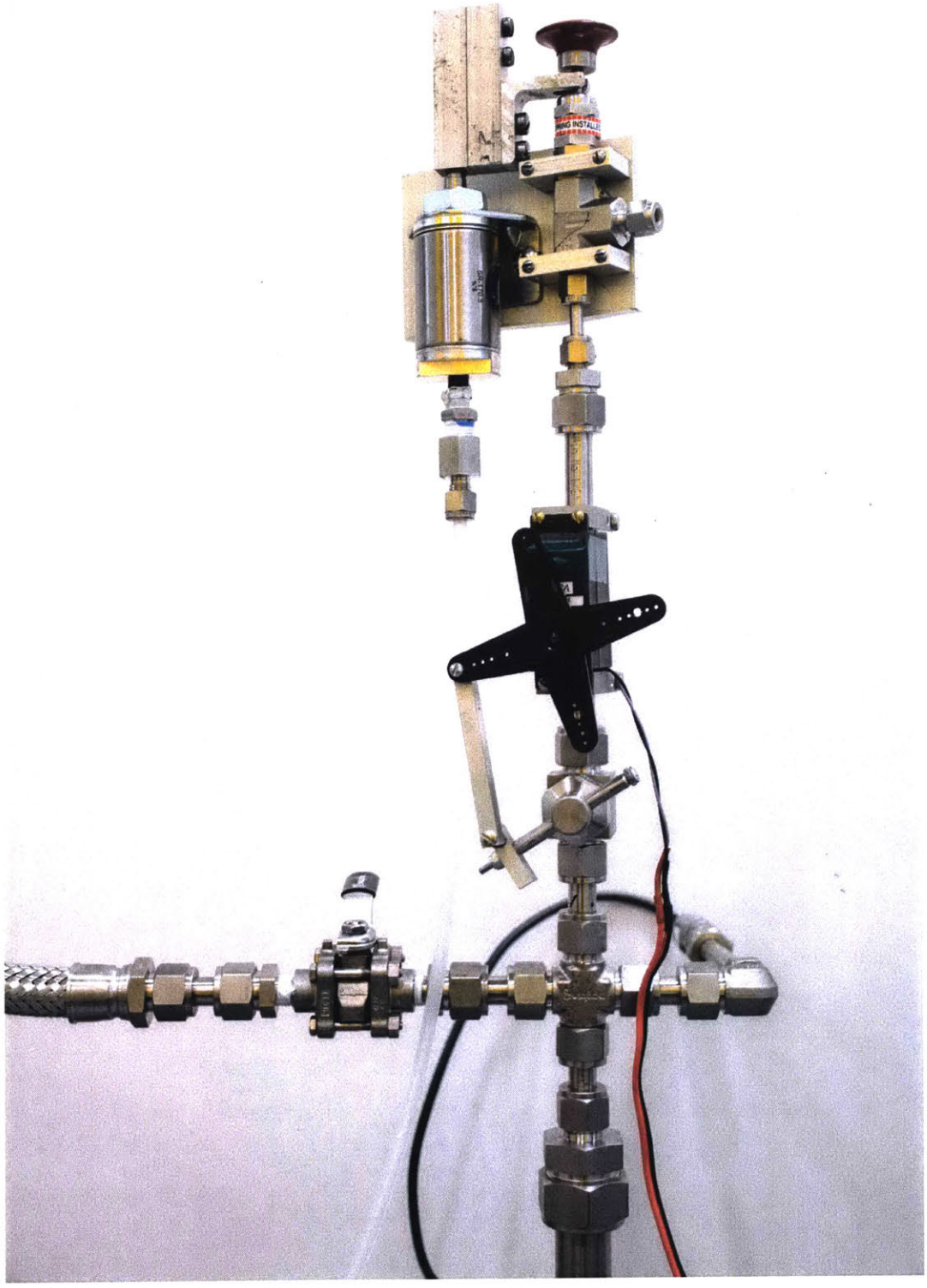

Figure A-4: Close up image of initiation and fail safe mechanisms together

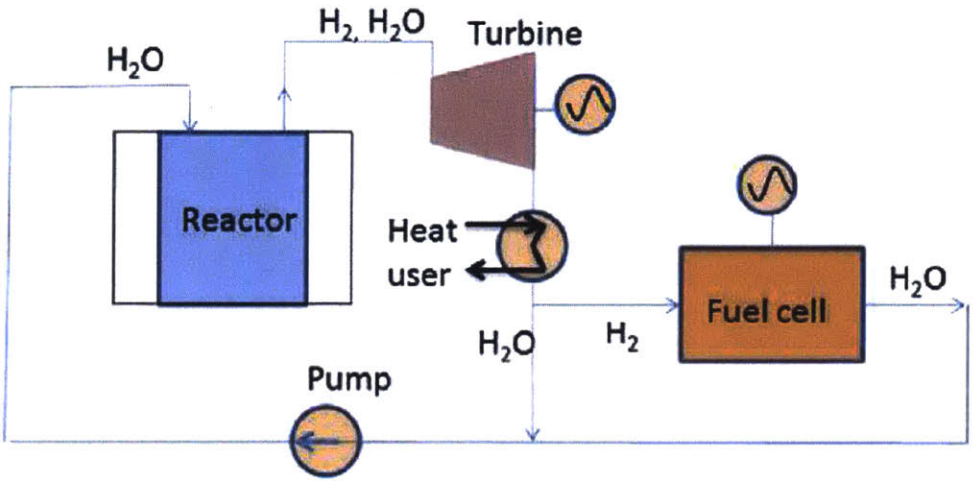

(a) OTL

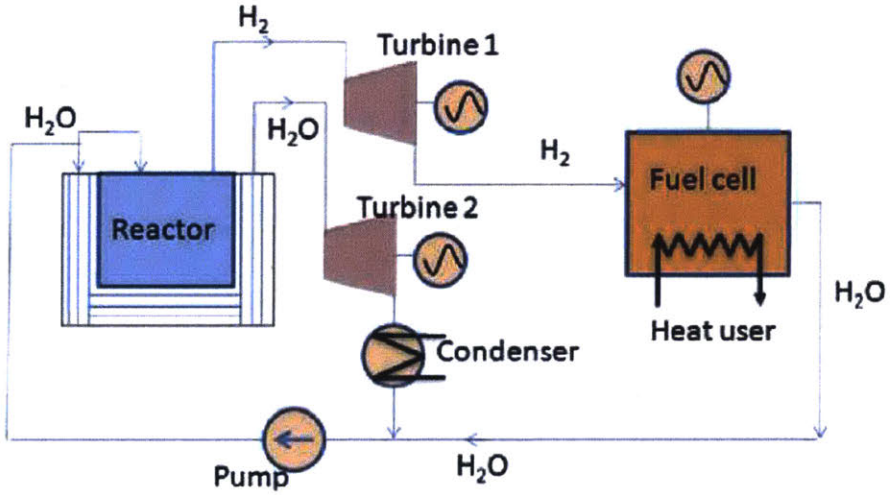

(b) TTL

Figure A-5: Heat recovery systems proposed in [26]

THIS PAGE INTENTIONALLY LEFT BLANK

Appendix B

Tables

Storage System Targets	**Gravimetric Density** kWh/kg system (kg H_2/kg system)	**Volumetric Density** kWh/L system (kg H_2/L system)	**Cost** $/kWh ($/kg H_2)
2020	1.8 (0.055)	1.3 (0.040)	$10 ($333)
Ultimate	2.5 (0.075)	2.3 (0.070)	$8 ($266)
Current Status (from Argonne National Laboratory)	**Gravimetric Density** kWh/kg system (kg H_2/kg system)	**Volumetric Density** kWh/L system (kg H_2/L system)	**Cost**[b] $/kWh ($/kg H_2)
700 bar compressed (Type IV, single tank)	1.5 (0.044)	0.8 (0.024)	$17[c] ($566)
350 bar compressed (Type IV, single tank)	1.8 (0.054)	0.6 (0.017)	$13[c] ($433)

[a] Assumes a storage capacity of 5.6 kg of usable hydrogen.

[b] Cost projections are estimated at 500,000 units per year and are reported in 2007$.

[c] Cost projection from Strategic Analysis (January 2013).

Table B.1: U.S. Department of Energy's reported current state of hydrogen energy and goals for hydrogen energy [5]

Temperature ($°C$)	237	258	280	296	303	310	319	331	339	344	359
Reaction time (s)	870	429	218	157	121	90	68	52	44	40	33
Conversion degree (%)	88	91	99	100	100	100	100	100	100	100	100

Table B.2: Reaction data for hydrothermal oxidation of aluminum to create $AlOOH$ in a very small scale production study [21]

Variable	Units	Description
G	$\frac{J}{mol}$	Gibbs free energy
H	$\frac{J}{mol}$	enthalpy
S	$\frac{J}{mol \cdot K}$	entropy
T	K	reaction operating temperature
P	Pa	pressure
V	m^3	system volume
ΔG	$\frac{J}{mol}$	change in free energy of the reaction per mole of Al reacted
ΔH	$\frac{J}{mol}$	change in enthalpy of the reaction per mole of Al reacted
ΔS	$\frac{J}{mol \cdot K}$	change in entropy of the reaction per mole of Al reacted
g	$\frac{J}{mol}$	specific free energy
h	$\frac{J}{mol}$	specific enthalpy
s	$\frac{J}{mol \cdot K}$	specific entropy
v	$\frac{m^3}{mol}$	specific volume
c_P	$\frac{J}{mol \cdot K}$	specific heat capacity
X		moles of steam produced in $Al(OH)_3$ reaction
Y		moles of steam produced in $AlOOH$ reaction
Z		moles of steam produced in Al_2O_3 reaction
PP_{H_2}	Pa	partial pressure of hydrogen
PP_{N_2}	Pa	partial pressure of nitrogen
PP_{H_2O}	Pa	partial pressure of steam
N_{H_2}	mol	number of moles of hydrogen
N_{N_2}	mol	number of moles of nitrogen
$N_{H_2O_{(g)}}$	mol	number of moles of steam
N_{tot}	mol	total number of moles in the system
R	$\frac{J}{mol \cdot K}$	universal gas constant $8.314 \frac{J}{mol \cdot K}$

Table B.3: Variables used in Chapter 2

Appendix C

Equations

$$\Delta H(T)_{Al(OH)_3} = -(1.0336 \cdot 10^{-4})(T^3) + (1.16339 \cdot 10^{-1})(T^2) - (1.48122 \cdot 10^{2})(T) - 3.99101 \cdot 10^{5} \quad \text{(C.1)}$$

$$\Delta H(T)_{AlOOH} = (1.65391 \cdot 10^{-5})(T^3) - (5.78315 \cdot 10^{-2})(T^2) - (3.1965 \cdot 10^{1})T - (4.06428 \cdot 10^{5}) \quad \text{(C.2)}$$

$$\Delta H(T)_{Al_2O_3} = -(1.33892 \cdot 10^{-5})(T^3) + (1.18306 \cdot 10^{-2})(T^2) - (5.42221 \cdot 10^{1})T - (3.93635 \cdot 10^{5}) \quad \text{(C.3)}$$

$$\Delta G(T)_{Al(OH)_3} = -(5.27486 \cdot 10^{-5})(T^3) + (1.92932 \cdot 10^{-1})(T^2) - (1.2644 \cdot 10^{2})T - 4.21972 \cdot 10^{5} \quad \text{(C.4)}$$

$$\Delta G(T)_{AlOOH} = -(3.1213 \cdot 10^{-5})(T^3) + (1.25031 \cdot 10^{-1})(T^2) - (1.28638 \cdot 10^{2})T - 4.11351 \cdot 10^{5} \quad \text{(C.5)}$$

$$\Delta G(T)_{Al_2O_3} = -(3.08926 \cdot 10^{-5})(T^3) + (1.00455 \cdot 10^{-1})(T^2) \\ -(1.3883 \cdot 10^2)T - 4.02071 \cdot 10^5 \quad \text{(C.6)}$$

Equations generated by FactSage courtesy of MIT's Department of Materials Science and Engineering [2].

Bibliography

[1] Energy density. https://en.wikipedia.org/wiki/Energy_density. Date Accessed: 01 November 2016.

[2] Factsage: The integrated thermodynamic databank system. MIT Department of Materials Science and Engineering. Date Accessed: 1 March 2017.

[3] Hydrogen storage. https://energy.gov/eere/fuelcells/hydrogen-storage. Date Accessed: 25 April 2017.

[4] Material considerations when working with hydrogen. http://www.hysafe.org/download/1002/BRHS%20Chap3%20-%20material%20consideration-version%201_0_1.pdf. Date Accessed: 1 May 2016.

[5] Physical hydrogen storage. https://energy.gov/eere/fuelcells/physical-hydrogen-storage. Date Accessed: 25 April 2017.

[6] Reaction of aluminum with water to produce hydrogen. *U.S. Department of Energy*, 2008.

[7] Hydrogen. http://www.afdc.energy.gov/fuels/hydrogen.html, May 10 2016. Date Accessed: 01 November 2016.

[8] L.V. Al'myashevea, E.N. Korytkova, A.V. Maslov, and V.V. Gusarov. Preparation of nanocrystalline alumina under hydrothermal conditions. *Inorganic Materials Journal*, 41(5):460–467, 2005. This is a full ARTICLE entry.

[9] U[lf] Bossel. Does a hydrogen economy make sense? *Proceedings of the IEEE*, 94(10):1826–1837, October 2006. This is a full ARTICLE entry.

[10] U[lf] Bossel and B[aldur] Eliasson. Energy and the hydrogen economy. Technical report, U.S. Department of Energy, Alternative Fuels Data Center, 2003.

[11] Z[hen-Yan] Deng and J[ose] M. F. Ferreira. Physicochemical mechanism for the continuous reaction of γ-al2o3-modified aluminum powder with water. *The American Ceramic Society Journal*, 90(5):1521–1526, May 2007. This is a full ARTICLE entry.

[12] M[athieu] Digne, P[hilippe] Sautet, P[ascal] Raybaud, H[erve] Toulhoat, and E[milio] Artacho. Structure and stability of aluminum hydroxides: A theoretical study. *Journal of Physical Chemistry*, 106:5155–5162, March 2002. This is a full ARTICLE entry.

[13] H. Elderfield and J. D. Hem. The development of crystalline structure in aluminum hyroxide polymorphs on ageing. *Mineralogical Magazine*, 39:89–96, March 1973. This is a full ARTICLE entry.

[14] S[hani] Elitzur, V[alery] Rosenband, and A[lon] Gany. Urine and aluminum as a source for hydrogen and clean energy. *International Journal of Hydrogen Energy*, 41:11909–11913, June 2016. This is a full ARTICLE entry.

[15] Ahmed Ghoniem. Advanced energy conversion. MIT Mechanical Engineering Lecture Presentation, February - May 2016.

[16] H[uihui] Huang, L[ei] Wang, Y[uan] Cai, C[aicheng] Zhou, Y[uewei] Yuan, X[iaojun] Zhang, H[ui] Wan, and G[uofeng] Guan. Facile fabrication of urchin-like hollow boehmite and alumina microspheres with a hierarchical structure via triton x-100 assisted hydrothermal systhesis. *CrystEngComm Journal*, 17:1318–1325, December 2014. This is a full ARTICLE entry.

[17] David Linden and Thomas B. Reddy. *Handbook of Batteries*. McGraw-Hill, 2002.

[18] A.S. Lozhkomoev, E.A. Glazkova, O.V. Bakina, M.I. Lerner, I. Gotman, E.Y. Gutmanas, S.O. Kazantsev, and S.G. Psakhie. Synthesis of core-shell alooh hollow nanospheres by reacting al nanoparticles with water. *Nanotechnology Journal*, 27, April 2016. This is a full ARTICLE entry.

[19] R[oy] E. McClean, H.H. Nelson, and M[ark] L. Campbell. Kinetics of the reactions $al^2p^0 + h_2o$ over an extended temperature range. *Journal of Physical Chemistry*, 97:9673–9676, June 1993. This is a full ARTICLE entry.

[20] K.A. Narh, V.P Dwivedi, J.M. Grow, A. Stana, and W.Y. Shih. The effect of liquid gallium on the strengths of stainless steel and thermoplastics. *Journal of Materials Science*, 33:329–337, July 1998. This is a full ARTICLE entry.

[21] E[vgeny] I. Shkolnikov, N[atalya] S. Shaitura, and M[ikhail] S. Vlaskin. Structural properties of boehmite produced by hydrothermal oxidation of aluminum. *The Journal of Supercritical Fluids*, 73:10–17, January 2013. This is a full ARTICLE entry.

[22] Jonathon Slocum. The design of a power system using treated aluminum fuel. Master's project, Massachusetts Institute of Technology, Department of Mechanical Engineering, May 2015. This is a full MASTERSTHESIS entry.

[23] N[ed] Stetson. Hydrogen storage program overview. *Department of Energy: Office of Energy Efficiency and Renewable Energy*, 2016.

[24] D. Tunega, H. Pasalic, M. H. Gerzabek, and H. Lischka. Theoretical study of structural, mechanical and spectroscopic properties of boehmite (γ-alooh). *Journal of Physics: Condensed Matter*, 23, September 2011. This is a full ARTICLE entry.

[25] E[isuke] Yamada, S[atoru] Watanabe, A. K. Hayashi, and N[obuyuki] Tsuiboi. Numerical analysis on auto-ignition of a high pressure hydrogen jet spouting from a tube. *Proceedings of the Combustion Institute Journal*, 32:2363–2369, July 2009. This is a full ARTICLE entry.

[26] W[eijuan] Yang, W[ei] Shi, C[hao] Chen, T[ianyou] Zhang, J[ianzhong] Liu, Z[hihua] Wang, and J[unhu] Zhou. Efficiency analysis of a novel electricity and heat co-generation system in the basis of aluminum-water reaction. *International Journal of Hydrogen Energy*, 42:3598–3604, September 2016. This is a full ARTICLE entry.